MIM-Refiner: A Contrastive Learning Boost from Intermediate Pre-Trained Representations

Benedikt Alkin[1,2] **Lukas Miklautz**[3] **Sepp Hochreiter**[1,2] **Johannes Brandstetter**[1,2]

[1] ELLIS Unit Linz, Institute for Machine Learning, JKU Linz, Austria
[2] NXAI GmbH, Linz, Austria
[3] Faculty of Computer Science, University of Vienna, Vienna, Austria
alkin@ml.jku.at

Abstract

We introduce MIM (Masked Image Modeling)-Refiner, a contrastive learning boost for pre-trained MIM models. MIM-Refiner is motivated by the insight that strong representations within MIM models generally reside in intermediate layers. Accordingly, MIM-Refiner leverages multiple contrastive heads that are connected to different intermediate layers. In each head, a modified nearest neighbor objective constructs semantic clusters that capture semantic information which improves performance on downstream tasks, including off-the-shelf and fine-tuning settings.
The refinement process is short and simple – yet highly effective. Within a few epochs, we refine the features of MIM models from subpar to state-of-the-art, off-the-shelf features. Refining a ViT-H, pre-trained with data2vec 2.0 on ImageNet-1K, sets a new state-of-the-art in linear probing (84.7%) and low-shot classification among models that are pre-trained on ImageNet-1K. MIM-Refiner efficiently combines the advantages of MIM and ID objectives and compares favorably against previous state-of-the-art SSL models on a variety of benchmarks such as low-shot classification, long-tailed classification, clustering and semantic segmentation. Project page: https://ml-jku.github.io/MIM-Refiner

1 Introduction

Self-supervised learning (SSL) has attracted considerable attention, owing to its data efficiency and generalization ability [49]. SSL leverages pre-training tasks and creates intricate input representations without the need for explicit supervision via expensive annotations. In computer vision, Masked Image Modeling (MIM) [12, 71, 58] has emerged as one of the prevalent SSL pre-training paradigms, enabling an efficient pretraining of large models on unlabeled data by reconstructing masked parts of the input images.

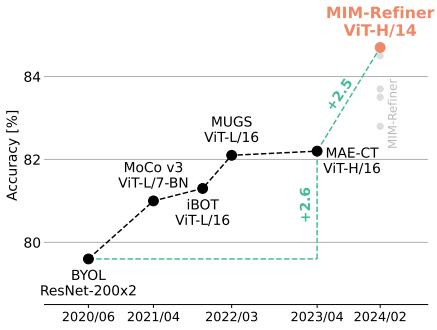

Figure 1: Linear probing state-of-the-art on ImageNet-1K over the last four years.

The success of MIM is driven by methods like Masked Autoencoder (MAE) [30], data2vec [7, 6], and others [8, 79]. For example, MAE opens the door for sparse pre-training of Vision Transformers (ViTs) [22] by masking large parts of the image and not processing the masked areas. The computational efficiency, coupled with the data efficiency of a generative reconstruction task [80, 25, 65] fosters the scaling to larger architectures on datasets of limited size. However, MIM models tend to spread their attention across the whole image [72]. When adapting to downstream tasks, a sufficient amount of labels is

38th Conference on Neural Information Processing Systems (NeurIPS 2024).

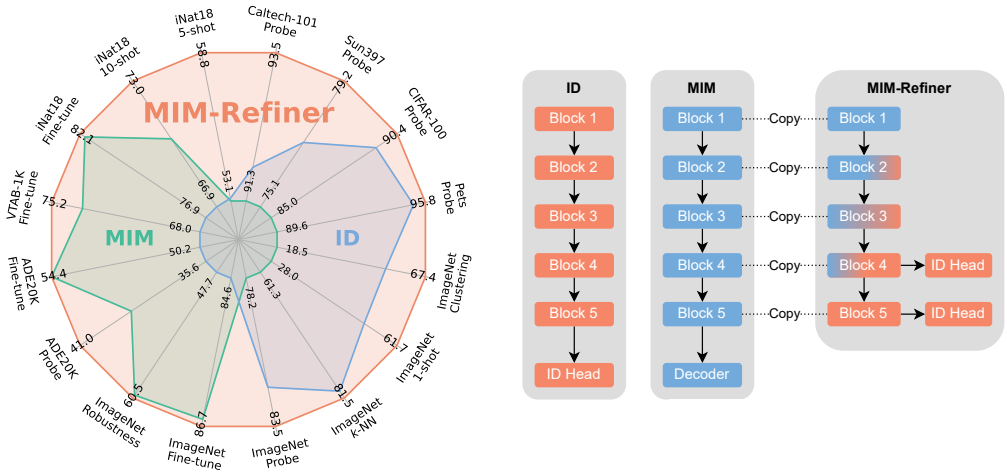

Figure 2: **Left:** Downstream evaluations of pre-trained SSL models. MIM-Refiner effectively combines their respective advantages of MIM and ID without suffering from their respective disadvantages. **Right:** Comparison of different pre-training schemes. ID uses a single ID head, whereas MIM models use a light-weight decoder to train an encoder. MIM-Refiner attaches multiple ID heads to the later third of the blocks of a pre-trained MIM encoder.

required to rewire the attention to focus on important regions in the image. In the absence thereof, MIM models perform poorly. In contrast, for example, Instance Discrimination (ID) [31, 14, 10, 29] methods implicitly focus on objects and form semantic clusters in the latent space [11], which eases adaption to downstream tasks in the absence of vast amounts of labels. In summary, the most important desiderata for efficient SSL pre-training methods in computer vision are rich representations of the input – ideally in the form of semantic clusters in the latent space – alongside efficiency in both compute and data, and, most notably, favorable scaling to larger architectures.

In this work, we first analyze pre-trained MIM models, where we find that MIM models have different types of blocks: those that mainly improve the pre-training objective and others that are responsible for abstraction within the MIM encoder. The origin of this behavior can be traced back to the fact that MIM architectures usually comprise a large ViT encoder together with a *very* light-weight decoder. For larger models, the light-weight decoder reaches a point, where it cannot further improve the pre-training objective on its own and passes part of the reconstruction task back to the last encoder blocks. Consequently, the feature quality for downstream tasks of the later blocks degrades, and, somewhat unusual, the representation quality peaks in the middle blocks of the encoder.

Based on these insights, we introduce MIM-Refiner, a simple – yet highly effective – sequential refinement approach tailored to MIM models. MIM-Refiner applies an ensemble of ID heads that enforce semantic clusters via an ID objective. Most importantly, those ID heads are attached to intermediate blocks of the encoder including those that exhibit peak representation quality, instead of only a single ID head attached to the last block.

Experimentally, we show that within few epochs, MIM-Refiner refines the features of a MIM model to (i) incorporate the beneficial properties of ID objectives (ii) preserves the advantages of the MIM model (iii) exploits the synergies of both methods to improve upon each individual pre-training objective, advancing the state-of-the-art across various benchmarks, see Figure 2.

2 Challenges of Masked Image Modeling

MIM models, such as MAE [30] and data2vec 2.0 [6], enable an efficient pre-training of large models. In terms of architecture, the encoder and decoder are intentionally designed asymmetrically. The encoder, on the one hand, is a large ViT, where discarding 75% of the input patches drastically reduces the cost of a forward pass. The decoder, on the other hand, operates on the full sequence length – by concatenating mask tokens to the encoded visible patches – and, thus, is typically *very* lightweight to compensate for the increased number of tokens (Figure 3a). As models increase in

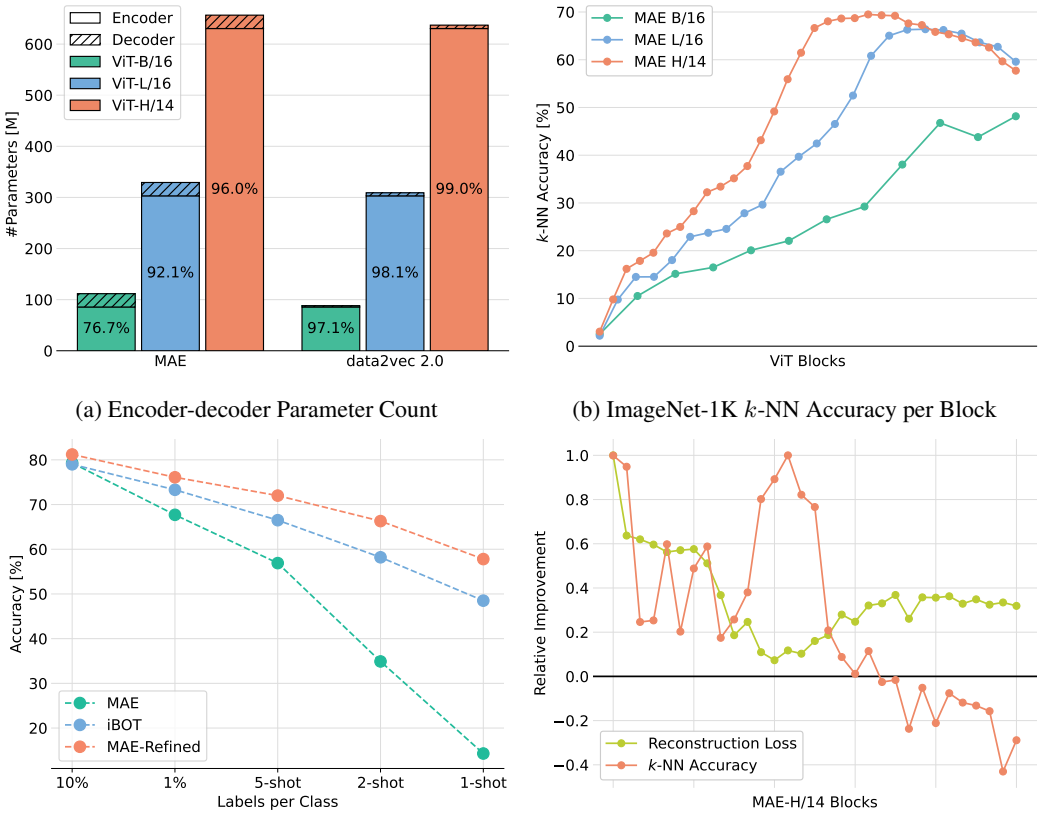

(a) Encoder-decoder Parameter Count

(b) ImageNet-1K k-NN Accuracy per Block

(c) ImageNet-1K Low-shot Accuracy.

(d) Relative Improvements per Block.

Figure 3: **(a)** MIM models are asymmetrically designed where the encoder has most of the parameters, as indicated by the percentages in the bars. **(b)** The representation quality of MAE encoders (measured by k-NN accuracy) peaks in the middle blocks before degrading when the later blocks take over parts of the decoder's task. Various MIM models and also a semantic segmentation task follow this pattern (see Appendix E.4) **(c)** The decline in representation quality in later blocks primarily contributes to the degradation in downstream performance. ID methods (represented by iBOT [86]) and our MAE-Refined do not suffer from this issue. **(d)** Correlation of the relative improvement of the reconstruction loss and the relative improvement in the k-NN accuracy per block. The relative k-NN accuracy improvement is obtained from the k-NN accuracy shown in **(b)**. Similarly, the relative improvement of the reconstruction loss is obtained from Figure 8 in the appendix. Middle blocks form abstract representations (large improvements in the k-NN accuracy, almost no improvement in reconstruction loss), later blocks take over parts of the reconstruction task (decrease in the k-NN accuracy, large improvement in the reconstruction loss). Additional details can be found in Appendix G.2.

size, the decoder eventually reaches a point where it cannot further improve the pre-training objective on its own. Consequently, it begins to delegate a portion of the reconstruction task back to the last encoder blocks. This transfer adversely affects the feature quality for downstream tasks associated with those blocks (Figure 3b), especially when only few labels are available (Figure 3c). We observe this phenomenon by correlating the relative improvement in the reconstruction loss vs the k-NN accuracy (Figure 3d). Roughly speaking, the blocks of the encoder operate in three different regimes:

1. In early ViT blocks, general purpose features are learned, which improve the reconstruction loss and the k-NN accuracy simultaneously.
2. In middle ViT blocks, abstractions are formed. The reconstruction loss improves only slightly, while the k-NN accuracy improves drastically.
3. In late ViT blocks, features are prepared for the reconstruction task. The reconstruction loss improves at a faster rate, while the k-NN accuracy decreases.

Table 1: Evaluating MIM-Refiner on a broad range of downstream tasks. "VTAB-6" reports the average accuracy over six datasets from the VTAB benchmark [83] and "VTAB-1K" is the average over all 19 datasets of the VTAB-1K benchmark. ADE20K reports the mean intersection over union (mIoU) of a semantic segmentation probe. MIM-Refiner learns strong general-purpose features that be readily used for various datasets and tasks. All models are pre-trained on ImageNet-1K [20]. "Probe" benchmarks and VTAB-6 train a linear layer on top of a frozen encoder using the full dataset. Other benchmarks fine-tune the encoder. See Appendix G for further implementation details.

		ImageNet		**iNat18**		**VTAB**		**ADE20K**
ViT	Method	5-shot	Probe	5-shot	Probe	VTAB-6	VTAB-1K	Probe
L/16	MAE	56.9	77.5	51.6	42.8	83.0	73.7	33.6
	iBOT	66.5	81.1	51.5	56.0	87.6	70.8	35.6
	Mugs	69.4	82.1	53.2	**61.5**	87.9	68.0	34.8
	MAE-Ref	**72.0**	**82.8**	**58.0**	60.6	**88.5**	**75.2**	**37.3**
H/14	MAE	40.2	78.2	53.3	43.0	83.2	72.7	35.5
	MAE-CT	67.4	82.3	60.1	62.8	88.8	75.7	37.6
	MAE-Ref	**73.8**	**83.7**	**62.4**	**64.6**	**89.3**	**75.9**	**39.4**
2B/14	MAE	62.9	79.7	53.7	51.0	85.4	74.1	37.3
	MAE-Ref	**74.8**	**84.5**	**63.5**	**69.6**	**89.8**	**75.6**	**40.3**

When naïvely using the features of the last encoder block, those features are suited for reconstruction, but not particularly for downstream tasks. If lots of labels are available, this can be compensated by fine-tuning the last encoder blocks on the downstream task. However, if not enough labels are available, or the last encoder blocks are not fine-tuned, downstream performance suffers.

One would think that simply using a larger decoder solves these problems. However, there are multiple problems with this solution. (i) The decoder commonly operates on the full sequence length, making it costly to increase its size. (ii) Scaling the decoder can decrease performance as shown, for example, in MAE [30] (Table 1). (iii) Models that can use a deeper decoder (such as CrossMAE [27]) also show degrading representation quality in later blocks, as shown in Appendix Figure 6d.

3 Method & Experiments

We propose MIM-Refiner, a novel approach aimed at improving downstream performance by refining the later blocks of a pre-trained MIM model. MIM-Refiner leverages the abstract intermediate representations with an ensemble of Instance Discrimination (ID) heads, which are attached to multiple blocks towards the end of the encoder, as visualized on the right side of Figure 2. As ID objective, we use Nearest Neighbor Alignment (NNA), which we introduce as a variant of NN-based ID methods [24, 4] to stabilize training of large-scale models (see Appendix B).

We refine MAE [30, 65] models, evaluate them on a variety of benchmarks and compare against state-of-the-art MIM and ID methods in Table 1. A comprehensive ablation study together with many more evaluations and additional refined MIM models can be found in Appendix C.

4 Conclusion

We introduce MIM-Refiner, a procedure to refine pre-trained MIM models. Motivated by the insights that the representation quality of MIM models peaks in the middle of the encoder, we employ an ensemble of instance discrimination heads attached at multiple blocks towards the end of the encoder, including the blocks where representation quality peaks, to improve upon the best existing representation. We train this ensemble for a short duration to improve the representation for downstream tasks such as classification, clustering or semantic segmentation.

Our refined MIM models learn strong features from ImageNet-1K alone that can be readily used for downstream tasks without fine-tuning the model but also improve performance when the model is fine-tuned, particularly in few-shot settings. Our models outperform competitors that were also trained on ImageNet-1K and sometimes also ones that were trained on more data or use larger models.

Acknowledgements

We thank Johannes Lehner for helpful discussions and suggestions.

We acknowledge EuroHPC Joint Undertaking for awarding us access to Karolina at IT4Innovations, Czech Republic, MeluXina at LuxProvide, Luxembourg, LUMI at CSC, Finland and Leonardo at CINECA, Italy. We acknowledge access to LEONARDO at CINECA, Italy, via an AURELEO (Austrian Users at LEONARDO supercomputer) project.

The ELLIS Unit Linz, the LIT AI Lab, the Institute for Machine Learning, are supported by the Federal State Upper Austria. We thank the projects Medical Cognitive Computing Center (MC3), INCONTROL-RL (FFG-881064), PRIMAL (FFG-873979), S3AI (FFG-872172), EPILEPSIA (FFG-892171), AIRI FG 9-N (FWF-36284, FWF-36235), AI4GreenHeatingGrids (FFG- 899943), INTEGRATE (FFG-892418), ELISE (H2020-ICT-2019-3 ID: 951847), Stars4Waters (HORIZON-CL6-2021-CLIMATE-01-01). We thank Audi.JKU Deep Learning Center, TGW LOGISTICS GROUP GMBH, Silicon Austria Labs (SAL), FILL Gesellschaft mbH, Anyline GmbH, Google, ZF Friedrichshafen AG, Robert Bosch GmbH, UCB Biopharma SRL, Merck Healthcare KGaA, Verbund AG, GLS (Univ. Waterloo), Software Competence Center Hagenberg GmbH, Borealis AG, TÜV Austria, Frauscher Sensonic, TRUMPF and the NVIDIA Corporation.

References

[1] Adaloglou, N., Michels, F., Kalisch, H., Kollmann, M.: Exploring the limits of deep image clustering using pretrained models. In: BMVC. pp. 297–299. BMVA Press (2023)

[2] Assran, M., Caron, M., Misra, I., Bojanowski, P., Bordes, F., Vincent, P., Joulin, A., Rabbat, M., Ballas, N.: Masked siamese networks for label-efficient learning. In: Avidan, S., Brostow, G.J., Cissé, M., Farinella, G.M., Hassner, T. (eds.) Computer Vision - ECCV 2022 - 17th European Conference, Tel Aviv, Israel, October 23-27, 2022, Proceedings, Part XXXI. Lecture Notes in Computer Science, vol. 13691, pp. 456–473. Springer (2022)

[3] Assran, M., Duval, Q., Misra, I., Bojanowski, P., Vincent, P., Rabbat, M.G., LeCun, Y., Ballas, N.: Self-supervised learning from images with a joint-embedding predictive architecture. In: IEEE/CVF Conference on Computer Vision and Pattern Recognition, CVPR 2023, Vancouver, BC, Canada, June 17-24, 2023. pp. 15619–15629. IEEE (2023)

[4] Azabou, M., Azar, M.G., Liu, R., Lin, C., Johnson, E.C., Bhaskaran-Nair, K., Dabagia, M., Hengen, K.B., Roncal, W.R.G., Valko, M., Dyer, E.L.: Mine your own view: Self-supervised learning through across-sample prediction. CoRR **abs/2102.10106** (2021)

[5] Bachlechner, T., Majumder, B.P., Mao, H.H., Cottrell, G., McAuley, J.J.: Rezero is all you need: fast convergence at large depth. In: de Campos, C.P., Maathuis, M.H., Quaeghebeur, E. (eds.) Proceedings of the Thirty-Seventh Conference on Uncertainty in Artificial Intelligence, UAI 2021, Virtual Event, 27-30 July 2021. Proceedings of Machine Learning Research, vol. 161, pp. 1352–1361. AUAI Press (2021)

[6] Baevski, A., Babu, A., Hsu, W., Auli, M.: Efficient self-supervised learning with contextualized target representations for vision, speech and language. In: Krause, A., Brunskill, E., Cho, K., Engelhardt, B., Sabato, S., Scarlett, J. (eds.) International Conference on Machine Learning, ICML 2023, 23-29 July 2023, Honolulu, Hawaii, USA. Proceedings of Machine Learning Research, vol. 202, pp. 1416–1429. PMLR (2023)

[7] Baevski, A., Hsu, W., Xu, Q., Babu, A., Gu, J., Auli, M.: data2vec: A general framework for self-supervised learning in speech, vision and language. In: ICML. Proceedings of Machine Learning Research, vol. 162, pp. 1298–1312. PMLR (2022)

[8] Bao, H., Dong, L., Piao, S., Wei, F.: Beit: BERT pre-training of image transformers. In: The Tenth International Conference on Learning Representations, ICLR 2022, Virtual Event, April 25-29, 2022. OpenReview.net (2022)

[9] Cai, Z., Ravichandran, A., Favaro, P., Wang, M., Modolo, D., Bhotika, R., Tu, Z., Soatto, S.: Semi-supervised vision transformers at scale. In: NeurIPS (2022)

[10] Caron, M., Misra, I., Mairal, J., Goyal, P., Bojanowski, P., Joulin, A.: Unsupervised learning of visual features by contrasting cluster assignments. In: Larochelle, H., Ranzato, M., Hadsell, R., Balcan, M., Lin, H. (eds.) Advances in Neural Information Processing Systems 33: Annual Conference on Neural Information Processing Systems 2020, NeurIPS 2020, December 6-12, 2020, virtual (2020)

[11] Caron, M., Touvron, H., Misra, I., Jégou, H., Mairal, J., Bojanowski, P., Joulin, A.: Emerging properties in self-supervised vision transformers. In: 2021 IEEE/CVF International Conference on Computer Vision, ICCV 2021, Montreal, QC, Canada, October 10-17, 2021. pp. 9630–9640. IEEE (2021)

[12] Chen, M., Radford, A., Child, R., Wu, J., Jun, H., Luan, D., Sutskever, I.: Generative pretraining from pixels. In: Proceedings of the 37th International Conference on Machine Learning, ICML 2020, 13-18 July 2020, Virtual Event. Proceedings of Machine Learning Research, vol. 119, pp. 1691–1703. PMLR (2020)

[13] Chen, M., Radford, A., Child, R., Wu, J., Jun, H., Luan, D., Sutskever, I.: Generative pretraining from pixels. In: ICML. Proceedings of Machine Learning Research, vol. 119, pp. 1691–1703. PMLR (2020)

[14] Chen, T., Kornblith, S., Norouzi, M., Hinton, G.E.: A simple framework for contrastive learning of visual representations. In: Proceedings of the 37th International Conference on Machine Learning, ICML 2020, 13-18 July 2020, Virtual Event. Proceedings of Machine Learning Research, vol. 119, pp. 1597–1607. PMLR (2020)

[15] Chen, X., Ding, M., Wang, X., Xin, Y., Mo, S., Wang, Y., Han, S., Luo, P., Zeng, G., Wang, J.: Context autoencoder for self-supervised representation learning. Int. J. Comput. Vis. **132**(1), 208–223 (2024)

[16] Cimpoi, M., Maji, S., Kokkinos, I., Mohamed, S., Vedaldi, A.: Describing textures in the wild. In: 2014 IEEE Conference on Computer Vision and Pattern Recognition, CVPR 2014, Columbus, OH, USA, June 23-28, 2014. pp. 3606–3613. IEEE Computer Society (2014)

[17] Clark, K., Luong, M., Le, Q.V., Manning, C.D.: ELECTRA: pre-training text encoders as discriminators rather than generators. In: 8th International Conference on Learning Representations, ICLR 2020, Addis Ababa, Ethiopia, April 26-30, 2020. OpenReview.net (2020)

[18] Cubuk, E.D., Zoph, B., Shlens, J., Le, Q.V.: Randaugment: Practical automated data augmentation with a reduced search space. In: 2020 IEEE/CVF Conference on Computer Vision and Pattern Recognition, CVPR Workshops 2020, Seattle, WA, USA, June 14-19, 2020. pp. 3008–3017. Computer Vision Foundation / IEEE (2020)

[19] Davies, D.L., Bouldin, D.W.: A cluster separation measure. IEEE Trans. Pattern Anal. Mach. Intell. **1**(2), 224–227 (1979)

[20] Deng, J., Dong, W., Socher, R., Li, L., Li, K., Fei-Fei, L.: Imagenet: A large-scale hierarchical image database. In: 2009 IEEE Computer Society Conference on Computer Vision and Pattern Recognition (CVPR 2009), 20-25 June 2009, Miami, Florida, USA. pp. 248–255. IEEE Computer Society (2009)

[21] Devlin, J., Chang, M., Lee, K., Toutanova, K.: BERT: pre-training of deep bidirectional transformers for language understanding. In: NAACL-HLT (1). pp. 4171–4186. Association for Computational Linguistics (2019)

[22] Dosovitskiy, A., Beyer, L., Kolesnikov, A., Weissenborn, D., Zhai, X., Unterthiner, T., Dehghani, M., Minderer, M., Heigold, G., Gelly, S., Uszkoreit, J., Houlsby, N.: An image is worth 16x16 words: Transformers for image recognition at scale. In: 9th International Conference on Learning Representations, ICLR 2021, Virtual Event, Austria, May 3-7, 2021. OpenReview.net (2021)

[23] Dosovitskiy, A., Fischer, P., Springenberg, J.T., Riedmiller, M.A., Brox, T.: Discriminative unsupervised feature learning with exemplar convolutional neural networks. IEEE Trans. Pattern Anal. Mach. Intell. **38**(9), 1734–1747 (2016)

[24] Dwibedi, D., Aytar, Y., Tompson, J., Sermanet, P., Zisserman, A.: With a little help from my friends: Nearest-neighbor contrastive learning of visual representations. In: 2021 IEEE/CVF International Conference on Computer Vision, ICCV 2021, Montreal, QC, Canada, October 10-17, 2021. pp. 9568–9577. IEEE (2021)

[25] El-Nouby, A., Izacard, G., Touvron, H., Laptev, I., Jégou, H., Grave, E.: Are large-scale datasets necessary for self-supervised pre-training? CoRR **abs/2112.10740** (2021)

[26] Fei-Fei, L., Fergus, R., Perona, P.: One-shot learning of object categories. IEEE transactions on pattern analysis and machine intelligence **28**(4), 594–611 (2006)

[27] Fu, L., Lian, L., Wang, R., Shi, B., Wang, X., Yala, A., Darrell, T., Efros, A.A., Goldberg, K.: Rethinking patch dependence for masked autoencoders. CoRR **abs/2401.14391** (2024)

[28] Gadetsky, A., Jiang, Y., Brbic, M.: Let go of your labels with unsupervised transfer. arXiv preprint arXiv:2406.07236 (2024)

[29] Grill, J., Strub, F., Altché, F., Tallec, C., Richemond, P.H., Buchatskaya, E., Doersch, C., Pires, B.Á., Guo, Z., Azar, M.G., Piot, B., Kavukcuoglu, K., Munos, R., Valko, M.: Bootstrap your own latent - A new approach to self-supervised learning. In: Larochelle, H., Ranzato, M., Hadsell, R., Balcan, M., Lin, H. (eds.) Advances in Neural Information Processing Systems 33: Annual Conference on Neural Information Processing Systems 2020, NeurIPS 2020, December 6-12, 2020, virtual (2020)

[30] He, K., Chen, X., Xie, S., Li, Y., Dollár, P., Girshick, R.B.: Masked autoencoders are scalable vision learners. In: Proceedings of the IEEE/CVF Conference on Computer Vision and Pattern Recognition, CVPR 2022. pp. 15979–15988 (2022)

[31] He, K., Fan, H., Wu, Y., Xie, S., Girshick, R.B.: Momentum contrast for unsupervised visual representation learning. In: 2020 IEEE/CVF Conference on Computer Vision and Pattern Recognition, CVPR 2020, Seattle, WA, USA, June 13-19, 2020. pp. 9726–9735. Computer Vision Foundation / IEEE (2020)

[32] Hendrycks, D., Basart, S., Mu, N., Kadavath, S., Wang, F., Dorundo, E., Desai, R., Zhu, T., Parajuli, S., Guo, M., Song, D., Steinhardt, J., Gilmer, J.: The many faces of robustness: A critical analysis of out-of-distribution generalization. ICCV (2021)

[33] Hendrycks, D., Dietterich, T.G.: Benchmarking neural network robustness to common corruptions and perturbations. In: ICLR (Poster). OpenReview.net (2019)

[34] Hendrycks, D., Gimpel, K.: Gaussian error linear units (gelus). arXiv preprint arXiv:1606.08415 (2016)

[35] Hendrycks, D., Zhao, K., Basart, S., Steinhardt, J., Song, D.: Natural adversarial examples. CVPR (2021)

[36] Horn, G.V., Aodha, O.M., Song, Y., Cui, Y., Sun, C., Shepard, A., Adam, H., Perona, P., Belongie, S.J.: The inaturalist species classification and detection dataset. In: 2018 IEEE Conference on Computer Vision and Pattern Recognition, CVPR 2018, Salt Lake City, UT, USA, June 18-22, 2018. pp. 8769–8778. Computer Vision Foundation / IEEE Computer Society (2018)

[37] Huang, G., Sun, Y., Liu, Z., Sedra, D., Weinberger, K.Q.: Deep networks with stochastic depth. In: Leibe, B., Matas, J., Sebe, N., Welling, M. (eds.) Computer Vision - ECCV 2016 - 14th European Conference, Amsterdam, The Netherlands, October 11-14, 2016, Proceedings, Part IV. Lecture Notes in Computer Science, vol. 9908, pp. 646–661. Springer (2016)

[38] Huang, Z., Jin, X., Lu, C., Hou, Q., Cheng, M., Fu, D., Shen, X., Feng, J.: Contrastive masked autoencoders are stronger vision learners. CoRR **abs/2207.13532** (2022)

[39] Hubert, L., Arabie, P.: Comparing partitions. Journal of classification **2**, 193–218 (1985)

[40] Ioffe, S., Szegedy, C.: Batch normalization: Accelerating deep network training by reducing internal covariate shift. In: Bach, F.R., Blei, D.M. (eds.) Proceedings of the 32nd International Conference on Machine Learning, ICML 2015, Lille, France, 6-11 July 2015. JMLR Workshop and Conference Proceedings, vol. 37, pp. 448–456. JMLR.org (2015)

[41] Jiang, Z., Chen, Y., Liu, M., Chen, D., Dai, X., Yuan, L., Liu, Z., Wang, Z.: Layer grafted pre-training: Bridging contrastive learning and masked image modeling for label-efficient representations. In: The Eleventh International Conference on Learning Representations, ICLR 2023, Kigali, Rwanda, May 1-5, 2023. OpenReview.net (2023)

[42] Kingma, D.P., Ba, J.: Adam: A method for stochastic optimization. In: Bengio, Y., LeCun, Y. (eds.) 3rd International Conference on Learning Representations, ICLR 2015, San Diego, CA, USA, May 7-9, 2015, Conference Track Proceedings (2015)

[43] Kirillov, A., Mintun, E., Ravi, N., Mao, H., Rolland, C., Gustafson, L., Xiao, T., Whitehead, S., Berg, A.C., Lo, W., Dollár, P., Girshick, R.B.: Segment anything. In: ICCV. pp. 3992–4003. IEEE (2023)

[44] Krizhevsky, A.: Learning multiple layers of features from tiny images (2009)

[45] Kvalseth, T.O.: Entropy and correlation: Some comments. IEEE Transactions on Systems, Man, and Cybernetics **17**(3), 517–519 (1987)

[46] Lee, C., Xie, S., Gallagher, P.W., Zhang, Z., Tu, Z.: Deeply-supervised nets. In: Lebanon, G., Vishwanathan, S.V.N. (eds.) Proceedings of the Eighteenth International Conference on Artificial Intelligence and Statistics, AISTATS 2015, San Diego, California, USA, May 9-12, 2015. JMLR Workshop and Conference Proceedings, vol. 38. JMLR.org (2015)

[47] Lehner, J., Alkin, B., Fürst, A., Rumetshofer, E., Miklautz, L., Hochreiter, S.: Contrastive tuning: A little help to make masked autoencoders forget. In: Thirty-Eighth AAAI Conference on Artificial Intelligence, AAAI 2024, February 20-27, 2024, Vancouver, Canada. pp. 2965–2973. AAAI Press (2024)

[48] Leiber, C., Miklautz, L., Plant, C., Böhm, C.: Benchmarking deep clustering algorithms with clustpy. In: ICDM (Workshops). pp. 625–632. IEEE (2023)

[49] Liu, X., Zhang, F., Hou, Z., Mian, L., Wang, Z., Zhang, J., Tang, J.: Self-supervised learning: Generative or contrastive. IEEE transactions on knowledge and data engineering **35**(1), 857–876 (2021)

[50] Liu, X., Zhou, J., Kong, T., Lin, X., Ji, R.: Exploring target representations for masked autoencoders. CoRR **abs/2209.03917** (2022)

[51] Loshchilov, I., Hutter, F.: Decoupled weight decay regularization. In: 7th International Conference on Learning Representations, ICLR 2019, New Orleans, LA, USA, May 6-9, 2019. OpenReview.net (2019)

[52] Mairal, J.: Cyanure: An open-source toolbox for empirical risk minimization for python, c++, and soon more. CoRR **abs/1912.08165** (2019)

[53] McInnes, L., Healy, J., Saul, N., Grossberger, L.: Umap: Uniform manifold approximation and projection. The Journal of Open Source Software **3**(29), 861 (2018)

[54] Nguyen, X.V., Epps, J., Bailey, J.: Information theoretic measures for clusterings comparison: is a correction for chance necessary? In: ICML. ACM International Conference Proceeding Series, vol. 382, pp. 1073–1080. ACM (2009)

[55] Nilsback, M.E., Zisserman, A.: Automated flower classification over a large number of classes. In: 2008 Sixth Indian conference on computer vision, graphics & image processing. pp. 722–729. IEEE (2008)

[56] Oquab, M., Darcet, T., Moutakanni, T., Vo, H., Szafraniec, M., Khalidov, V., Fernandez, P., Haziza, D., Massa, F., El-Nouby, A., Assran, M., Ballas, N., Galuba, W., Howes, R., Huang, P., Li, S., Misra, I., Rabbat, M.G., Sharma, V., Synnaeve, G., Xu, H., Jégou, H., Mairal, J., Labatut, P., Joulin, A., Bojanowski, P.: Dinov2: Learning robust visual features without supervision. CoRR **abs/2304.07193** (2023)

[57] Parkhi, O.M., Vedaldi, A., Zisserman, A., Jawahar, C.V.: Cats and dogs. In: 2012 IEEE Conference on Computer Vision and Pattern Recognition, Providence, RI, USA, June 16-21, 2012. pp. 3498–3505. IEEE Computer Society (2012)

[58] Pathak, D., Krähenbühl, P., Donahue, J., Darrell, T., Efros, A.A.: Context encoders: Feature learning by inpainting. In: 2016 IEEE Conference on Computer Vision and Pattern Recognition, CVPR 2016, Las Vegas, NV, USA, June 27-30, 2016. pp. 2536–2544. IEEE Computer Society (2016)

[59] Pedregosa, F., Varoquaux, G., Gramfort, A., Michel, V., Thirion, B., Grisel, O., Blondel, M., Prettenhofer, P., Weiss, R., Dubourg, V., VanderPlas, J., Passos, A., Cournapeau, D., Brucher, M., Perrot, M., Duchesnay, E.: Scikit-learn: Machine learning in python. J. Mach. Learn. Res. **12**, 2825–2830 (2011)

[60] Polyak, B.T., Juditsky, A.B.: Acceleration of stochastic approximation by averaging. SIAM journal on control and optimization **30**(4), 838–855 (1992)

[61] Radford, A., Kim, J.W., Hallacy, C., Ramesh, A., Goh, G., Agarwal, S., Sastry, G., Askell, A., Mishkin, P., Clark, J., Krueger, G., Sutskever, I.: Learning transferable visual models from natural language supervision. In: Meila, M., Zhang, T. (eds.) Proceedings of the 38th International Conference on Machine Learning, ICML 2021, 18-24 July 2021, Virtual Event. Proceedings of Machine Learning Research, vol. 139, pp. 8748–8763. PMLR (2021)

[62] Radford, A., Narasimhan, K., Salimans, T., Sutskever, I., et al.: Improving language understanding by generative pre-training (2018)

[63] Rousseeuw, P.J.: Silhouettes: a graphical aid to the interpretation and validation of cluster analysis. Journal of computational and applied mathematics **20**, 53–65 (1987)

[64] Sculley, D.: Web-scale k-means clustering. In: WWW. pp. 1177–1178. ACM (2010)

[65] Singh, M., Duval, Q., Alwala, K.V., Fan, H., Aggarwal, V., Adcock, A., Joulin, A., Dollár, P., Feichtenhofer, C., Girshick, R.B., Girdhar, R., Misra, I.: The effectiveness of MAE pre-pretraining for billion-scale pretraining. CoRR **abs/2303.13496** (2023)

[66] Singh, M., Gustafson, L., Adcock, A., de Freitas Reis, V., Gedik, B., Kosaraju, R.P., Mahajan, D., Girshick, R.B., Dollár, P., van der Maaten, L.: Revisiting weakly supervised pre-training of visual perception models. In: IEEE/CVF Conference on Computer Vision and Pattern Recognition, CVPR 2022, New Orleans, LA, USA, June 18-24, 2022. pp. 794–804. IEEE (2022)

[67] Szegedy, C., Liu, W., Jia, Y., Sermanet, P., Reed, S.E., Anguelov, D., Erhan, D., Vanhoucke, V., Rabinovich, A.: Going deeper with convolutions. In: IEEE Conference on Computer Vision and Pattern Recognition, CVPR 2015, Boston, MA, USA, June 7-12, 2015. pp. 1–9. IEEE Computer Society (2015)

[68] Szegedy, C., Vanhoucke, V., Ioffe, S., Shlens, J., Wojna, Z.: Rethinking the inception architecture for computer vision. In: 2016 IEEE Conference on Computer Vision and Pattern Recognition, CVPR 2016, Las Vegas, NV, USA, June 27-30, 2016. pp. 2818–2826. IEEE Computer Society (2016)

[69] Touvron, H., Cord, M., Sablayrolles, A., Synnaeve, G., Jégou, H.: Going deeper with image transformers. In: 2021 IEEE/CVF International Conference on Computer Vision, ICCV 2021, Montreal, QC, Canada, October 10-17, 2021. pp. 32–42. IEEE (2021)

[70] Vaswani, A., Shazeer, N., Parmar, N., Uszkoreit, J., Jones, L., Gomez, A.N., Kaiser, L., Polosukhin, I.: Attention is all you need. In: NIPS. pp. 5998–6008 (2017)

[71] Vincent, P., Larochelle, H., Lajoie, I., Bengio, Y., Manzagol, P.: Stacked denoising autoencoders: Learning useful representations in a deep network with a local denoising criterion. J. Mach. Learn. Res. **11**, 3371–3408 (2010)

[72] Walmer, M., Suri, S., Gupta, K., Shrivastava, A.: Teaching matters: Investigating the role of supervision in vision transformers. In: CVPR. pp. 7486–7496. IEEE (2023)

[73] Wang, H., Ge, S., Lipton, Z., Xing, E.P.: Learning robust global representations by penalizing local predictive power. In: Advances in Neural Information Processing Systems. pp. 10506–10518 (2019)

[74] Wang, L., Liang, F., Li, Y., Zhang, H., Ouyang, W., Shao, J.: Repre: Improving self-supervised vision transformer with reconstructive pre-training. In: Raedt, L.D. (ed.) Proceedings of the Thirty-First International Joint Conference on Artificial Intelligence, IJCAI 2022, Vienna, Austria, 23-29 July 2022. pp. 1437–1443. ijcai.org (2022)

[75] Wei, C., Fan, H., Xie, S., Wu, C., Yuille, A.L., Feichtenhofer, C.: Masked feature prediction for self-supervised visual pre-training. In: CVPR. pp. 14648–14658. IEEE (2022)

[76] Wu, Z., Xiong, Y., Yu, S.X., Lin, D.: Unsupervised feature learning via non-parametric instance discrimination. In: 2018 IEEE Conference on Computer Vision and Pattern Recognition, CVPR 2018, Salt Lake City, UT, USA, June 18-22, 2018. pp. 3733–3742. Computer Vision Foundation / IEEE Computer Society (2018)

[77] Xiao, J., Hays, J., Ehinger, K.A., Oliva, A., Torralba, A.: SUN database: Large-scale scene recognition from abbey to zoo. In: The Twenty-Third IEEE Conference on Computer Vision and Pattern Recognition, CVPR 2010, San Francisco, CA, USA, 13-18 June 2010. pp. 3485–3492. IEEE Computer Society (2010)

[78] Xiao, T., Liu, Y., Zhou, B., Jiang, Y., Sun, J.: Unified perceptual parsing for scene understanding. In: Ferrari, V., Hebert, M., Sminchisescu, C., Weiss, Y. (eds.) Computer Vision - ECCV 2018 - 15th European Conference, Munich, Germany, September 8-14, 2018, Proceedings, Part V. Lecture Notes in Computer Science, vol. 11209, pp. 432–448. Springer (2018)

[79] Xie, Z., Zhang, Z., Cao, Y., Lin, Y., Bao, J., Yao, Z., Dai, Q., Hu, H.: Simmim: a simple framework for masked image modeling. In: IEEE/CVF Conference on Computer Vision and Pattern Recognition, CVPR 2022, New Orleans, LA, USA, June 18-24, 2022. pp. 9643–9653. IEEE (2022)

[80] Xie, Z., Zhang, Z., Cao, Y., Lin, Y., Wei, Y., Dai, Q., Hu, H.: On data scaling in masked image modeling. In: Proceedings of the IEEE/CVF Conference on Computer Vision and Pattern Recognition. pp. 10365–10374 (2023)

[81] Yang, Y., Xu, D., Nie, F., Yan, S., Zhuang, Y.: Image clustering using local discriminant models and global integration. IEEE Transactions on Image Processing **19**(10), 2761–2773 (2010)

[82] Yi, K., Ge, Y., Li, X., Yang, S., Li, D., Wu, J., Shan, Y., Qie, X.: Masked image modeling with denoising contrast. In: The Eleventh International Conference on Learning Representations, ICLR 2023, Kigali, Rwanda, May 1-5, 2023. OpenReview.net (2023)

[83] Zhai, X., Puigcerver, J., Kolesnikov, A., Ruyssen, P., Riquelme, C., Lucic, M., Djolonga, J., Pinto, A.S., Neumann, M., Dosovitskiy, A., et al.: A large-scale study of representation learning with the visual task adaptation benchmark. arXiv preprint arXiv:1910.04867 (2019)

[84] Zhang, H., Cissé, M., Dauphin, Y.N., Lopez-Paz, D.: mixup: Beyond empirical risk minimization. In: 6th International Conference on Learning Representations, ICLR 2018, Vancouver, BC, Canada, April 30 - May 3, 2018, Conference Track Proceedings. OpenReview.net (2018)

[85] Zhou, B., Zhao, H., Puig, X., Xiao, T., Fidler, S., Barriuso, A., Torralba, A.: Semantic understanding of scenes through the ADE20K dataset. Int. J. Comput. Vis. **127**(3), 302–321 (2019)

[86] Zhou, J., Wei, C., Wang, H., Shen, W., Xie, C., Yuille, A.L., Kong, T.: ibot: Image BERT pre-training with online tokenizer. CoRR **abs/2111.07832** (2021)

[87] Zhou, P., Zhou, Y., Si, C., Yu, W., Ng, T.K., Yan, S.: Mugs: A multi-granular self-supervised learning framework. CoRR **abs/2203.14415** (2022)

A Related Work

A.1 Pre-training in Computer Vision

Following the success of generative pre-training of transformers [70] in language modeling [21, 62], similar directions were explored in computer vision [22, 79, 75, 13]. With the introduction of Vision Transformers [22], large Masked Image Modeling (MIM) models could be efficiently trained [30, 6, 65] by using the ability of transformers to effortlessly process sparse input by dropping masked patch tokens in the input and subsequently reconstructing the masked parts. In order to optimize the MIM pre-training objective, models have to infer the missing regions by efficiently encoding foreground and background alike which leads to a rich representation.

Building on rich features learned by MIM models has been explored in various ways. MAWS [65] first pre-trains an MAE, followed by weakly supervised training on a billion-scale dataset using billion-scale models. SemiViT [9] uses a pre-trained MAE as a starting point for semi-supervised learning. Segment Anything [43] use MAE as basis for a segmentation foundation model. MIM-Refiner also builds on the rich features of MIM models and refines them with a ID objective to ease adaption to downstream tasks.

Instance Discrimination (ID) is another branch of self-supervised learning that uses augmentations to create multiple views of the same sample where the task is then to find matching pairs within the views from all samples within a batch [14, 31, 23, 76] or align features of one view with the features from another [29, 11]. We use the terminology that views from the same sample are "positive pairs" and views of different samples are "negative pairs". When describing a single view of a sample, it is called the "anchor" to which all other views in a batch are either "positives" or "negatives". NN-based ID [24, 4] extends this setting to use NNs in various ways to create views or otherwise augment samples during training. MIM-Refiner introduces Nearest Neighbor Alignment, which is a modification of previous NN-based ID methods to use the NN only for the alignment part, i.e. pulling the anchor closer to the NN of its positives while pushing the anchor away from its negatives.

A.2 Combining MIM and ID

Adding a MIM to ID methods has emerged as a powerful pre-training scheme. However, in contrast to ID models, the MIM objective in the end-to-end training either uses significantly lower masking ratios with mask tokens getting processed by the encoder [86, 56], or requires a target encoder to encode the unmasked image [38, 2]. Both *drastically* increase the computational requirements as the encoder operates on the full sequence length. Consequently, these models either require copious amounts of compute to train [56] or limit themselves to relatively small models [86, 38]. Contrary, MIM models have shown success and scalability to large models with comparatively little compute [30, 6, 65]. MIM-Refiner can build on these models which allows us to scale to large model sizes without a large amount of compute. Our largest model, MAE-Refined-2B contains approximately twice the parameters of the currently largest uni-modal contrastive model DINOv2-g [56] and can be trained on two orders of magnitude less data.

Attempts to preserve the efficiency while training MIM and ID objectives end-to-end have been less successful [47, 41], where both works came to the conclusion that sequential training (MIM $\rightarrow$ ID) circumvents various problem with end-to-end training. First, a powerful encoder is trained solely with a MIM objective. Second, the encoder is trained with a ID objective while preserving the rich features in early blocks with a layer-wise learning rate decay [17] in lower blocks and either constraining changes in early blocks [41] or completely freezing them [47].

MIM-Refiner is also a sequential MIM $\rightarrow$ ID method. In contrast to our work, previous works start from the representation after the last MIM encoder block and are therefore highly reliant on a good representation thereof. This can be seen for example on MAE-CT [47] where their ViT-H/14 model is worse than their ViT-H/16 model, despite using 30% more FLOPS. Additionally, previous works [47, 41] omit current go-to techniques such as multi-crop augmentation [10] which has been shown to improve performance [11, 87, 86].

Training models with additional losses from intermediate layers dates back to the early deep learning days [46, 67] where these auxiliary losses were used to alleviate optimization issues in lower layers. MIM-Refiner relates to deep supervision in the sense that we use multiple ID heads attached at intermediate layers where each head produces a loss for training.

B Nearest Neighbor Alignment Objective

In addition to the method described in Section 3, we propose an adapted ID objective to stabilize training of larger models. Inspired by NN based contrastive learning [24, 4], we propose Nearest Neighbor Alignment (NNA). NN contrastive objectives introduce an inter-sample correlation by retrieving NNs of samples in a batch and subsequently applying an objective between the samples and their NNs. In practice, the NN retrieval is typically done by tracking samples from previous iterations in a first-in-first-out queue [24, 31]. Therefore, the samples in the queue are from a previous model state which creates a tradeoff between the benefit of the NN-swap and the worse signal from the out-of-sync samples. We argue that the NN-swap does not offer a benefit for negative samples, since they are already different images, and instead, degrades the signal from the contrastive objective. We therefore propose to use the NN only for the alignment of positive samples. Omitting the NN-swap for the negatives stabilizes training for large models and slightly improves performance (see Table 2). NNA is a variant of NNCLR and we visualize their difference in Figure 10.

Formally, given a batch of features $\mathcal{Z} = \{z_1, \dots, z_N\}$ and a queue $\mathcal{Q}$ the NNA objective is:

$$\mathcal{L}_i^{\text{NNA}} = -\log \frac{\exp(\text{NN}(z_i, \mathcal{Q}) \cdot z_i/\tau)}{\exp(\text{NN}(z_i, \mathcal{Q}) \cdot z_i/\tau) + \sum_{j=1}^{N} \exp(\text{SG}(z_j) \cdot z_i/\tau)[i \neq j]} \tag{1}$$

$$\text{NN}(z_i, \mathcal{Q}) = \underset{q \in \mathcal{Q}}{\text{argmax}}(z_i \cdot q) \tag{2}$$

where z_i is the anchor, $\text{NN}(z_i, \mathcal{Q})$ is the positive, z_j are the negatives, τ is the temperature, and SG is the stop-gradient operation. $[i \neq j]$ denotes the Iverson bracket that evaluates to 1 if $i \neq j$ and to 0 if $i = j$. All vectors are assumed to be normalized to length 1.

C Comprehensive Experimental Evaluation

We refine a series of MIM models, namely MAE [30, 65], data2vec 2.0 [6] (abbreviated as D2V2), dBOT [50] and CrossMAE [27]. These models were pre-trained on ImageNet-1K [20], which we also use for the refinement. For visual clarity, we compare our best model against previous state-of-the-art models and show the full result tables in the Appendix. We evaluate our models in classification (low- and many-shot), feature evaluation, clustering, transfer learning and semantic segmentation.

C.1 Ablation Study

We first investigate various design choices of our method in Table 2.

(a) Adding **multiple heads** at intermediate features improves k-NN accuracy by 0.8%. The best settings include the blocks with the best representation quality (see Figure 3b). Adding additional heads before the best blocks does not improve performance while increasing training costs. (b) The benefit **doubles to 1.6% for a ViT-H** since deeper models degrade more (see Figure 3b). Additionally, we investigate where to attach the ID heads in Appendix E.2 where we find that simply attaching ID head to the last 8 (or 12 for ViT-H) blocks to perform best across model scales.

(c) **Scheduling the loss weight** of each intermediate head is not necessary, i.e. simply summing all losses is sufficient to achieve good performances. "Uniform Decay" decays the loss weight of all intermediate heads during training. "Staggered Decay" starts by decaying the first head and gradually starts to decay more and more heads as training progresses. "Staggered Step" disables the first head after some time followed by gradually disabling more and more heads. "One Hot" trains the encoder with only one intermediate head at a time where training starts with the earliest intermediate head and gradually iterates through the heads. Details to the loss schedules are in Appendix G.14.

(d) Using the **NN swap** only for aligning the positive with the anchor gives a small but consistent improvement on smaller models. (e) The improved signal quality is **cruicial to avoid training instabilities** in larger models. These instabilities manifest in a sudden representation quality drop mid-training leading to a much worse final model.

(f) Relying only on the data-driven **augmentation** of the NN-swap [24] by omitting color/blur augmentations, is beneficial for certain downstream tasks such as extreme low-shot classification [47]. We show more results without color/blur augmentations in Appendix E.5.

Table 2: Ablation study by refining data2vec 2.0 [6] models. Default settings

(a) **Head Count L/16**

#Heads	k-NN
1	80.2
2	80.2
4	80.9
8	**81.0**
12	**81.0**

(b) **Head Count H/14**

#Heads	k-NN
1	80.7
2	81.1
4	81.7
8	82.1
12	**82.3**

(c) **Head Schedule L/16**

Schedule	k-NN
Constant	**81.0**
Uniform Decay	80.9
Staggered Decay	**81.0**
Staggered Step	80.9
One Hot	80.7

(d) **NN-swap L/16**

Swap Neg.	k-NN
✗	**81.0**
✓	80.9

(e) **NN-swap H/14**

Swap Neg.	k-NN
✗	**82.3**
✓	80.7

(f) **Augmentations L/16**

Color/blur	k-NN	1-shot
✓	**81.0**	61.7
✗	80.5	**63.4**

C.2 Low-shot and Feature Evaluations

We evaluate the ability of our models to perform low-shot classification in Table 3. Additionally, linear probing and k-NN accuracy are reported which are computed from the features of the frozen encoder. These metrics are typically correlated to low-shot performance as it indicates that the representation is already linear separable which eases drawing decision boundaries given only few labels. For linear probing, we use the protocol of DINOv2 [56] which includes using features of the last four blocks in its hyperparameter grid. Therefore, linear probing evaluates the feature representation at the end of the encoder, while k-NN accuracy evaluates only the features of the last block.

MIM-Refiner drastically improves upon MIM models and other SSL models. In the 1-shot settings D2V2-Refined-H sets a new state-of-the-art of 64.2%, outperforming the 63.6% of MAWS-6.5B [65] which is pre-trained on a private dataset with approximately 2000 times the size of ImageNet-1K.

Table 3: Low-shot and feature evaluations of recent SSL models on ImageNet-1K. MIM-Refiner significantly improves upon MIM models and previous state-of-the-art SSL models. Appendix Table 11 extends this comparison to more methods and to models that were trained on more data (such as DINOv2) where MIM-Refiner outperforms DINOv2-g in some benchmarks.

		Low-shot Evaluation					**Feature Eval**	
ViT	Method	1-shot	2-shot	5-shot	1%	10%	Probe	k-NN
L/16	MAE [30]	14.3	34.9	56.9	67.7	79.3	77.5	60.6
	D2V2 [6]	24.1	58.8	72.1	75.1	81.5	78.2	51.8
	iBOT [86]	48.5	58.2	66.5	73.3	79.0	81.1	78.0
	Mugs [87]	52.9	62.3	69.4	76.2	80.3	82.1	80.4
	MAE-Refined	57.8	66.3	72.0	76.1	81.2	82.8	**81.5**
	D2V2-Refined	**61.7**	**69.6**	**73.9**	**78.1**	**82.1**	**83.5**	81.0
H/14	MAE [30]	7.2	14.1	40.2	72.8	81.2	78.2	58.1
	D2V2 [6]	21.6	60.8	74.2	77.6	83.3	80.4	48.0
	MAE-CT [47]	49.4	59.6	67.4	74.4	81.7	82.3	79.1
	MAE-Refined	59.5	68.5	73.8	77.4	82.1	83.7	**82.3**
	D2V2-Refined	**64.2**	**71.3**	**75.5**	**78.1**	**83.5**	**84.7**	**82.3**
2B/14	MAE [30, 65]	17.8	29.1	62.9	73.6	82.0	79.7	67.1
	MAE-Refined	**58.2**	**68.6**	**74.8**	**78.7**	**82.5**	**84.5**	**83.2**

C.3 Cluster Evaluations

We compare the cluster performance of MIM-Refiner against recent SSL models in Table 4. We apply mini-batch k-means [64] 100 times to the validation set of ImageNet-1K and select the run with the lowest k-means loss for comparison (average performance is reported in Appendix Table 13). We report commonly used metrics for measuring *Cluster Performance* w.r.t. the ground truth

Table 4: k-means cluster performance and class separation on ImageNet of recent SSL models. MIM-Refiner drastically improves performance of MIM-models and even outperforms DINOv2-g which has 2x more parameters and is trained on on 100x more data.

		Cluster Performance				**Class Separation**	
ViT	Method	ACC	NMI	AMI	ARI	SIL (↑)	DBS (↓)
L/16	D2V2 [6]	10.5	45.1	19.5	2.5	-9.1	6.4
	iBOT [86]	52.2	80.5	67.0	33.4	13.3	3.5
	Mugs [87]	54.3	78.6	65.5	22.4	14.9	3.3
	D2V2-Refined	**67.4**	**86.3**	**76.2**	**40.5**	**37.1**	**2.2**
H/14	D2V2 [6]	9.9	45.8	18.0	2.6	-10.8	6.5
	D2V2-Refined	**67.3**	**87.2**	**77.9**	**42.2**	**34.5**	**2.3**
H/16	MAE-CT	58.0	81.8	69.3	36.8	-	-
g/14	DINOv2 [56] (LVD-142M)	47.7	76.3	63.6	5.1	30.4	2.8

ACC: 19.3 | SIL: -12.2 (a) D2V2

ACC: 70.3 | SIL: 32.4 (b) D2V2-Refined

ACC: 64.3 | SIL: 10.0 (c) Mugs

Figure 4: UMAP [53] plots of ViT-L embeddings using all 53 food related classes of ImageNet. The corresponding k-means cluster accuracy (ACC) and class separation measured in silhouette score (SIL) is shown below each plot. The clustering after refinement (b) is visually more condensed and better separated with corresponding improvements in ACC and SIL than before refinement (a). Mugs **(c)** does not separate the clusters that well, as shown by the merged clusters in the middle and the lower SIL score. The colors show the 53 ground truth food classes.

clustering: Cluster Accuracy (ACC) [81], Normalized Mutual Information (NMI) [45], Adjusted Mutual Information (AMI) [54], Adjusted Rand Index (ARI) [39], where higher values indicate a better match of the found clustering with the ground truth labels. Further, we measure the *Class Separation* in the embedded space using the Davies-Bouldin score (DBS) [19] and silhouette score (SIL) [63] w.r.t. the ground truth classes. The DBS measures the separation and compactness of classes, where lower values are better and zero is the minimum. The SIL ranges from -100 to 100, where higher values are better. Negative SILs relate to mismatches between classes and embedding, where scores close to zero indicate a potential overlap of classes.

Table 4 shows that MIM-Refiner greatly improves various clustering metrics. The reached ACC of 67.4% outperforms the current state-of-the-art of 61.6% reached by TEMI MSN [1]. Figure 4 illustrate this drastic increase in cluster performance and class separation visually. Additionally, we evaluate combining multiple models using the TURTLE [28] framework in Appendix Table 14.

C.4 Transfer Learning Evaluations

We investigate generalization of pre-trained MIM-Refiner models to other datasets in Table 5, which shows the benefits of MIM-Refiner models when transferring a pre-trained representation. We consider a variety of classification downstream tasks and a semantic segmentation task. MAE-Refined consistently improves over MAE and state-of-the-art SSL methods. Additionally MIM-Refiner further improves when scaling up to a 2B parameter model.

Table 5: Transferring MIM-Refiner models to other datasets. "VTAB-6" reports the average accuracy over six datasets from the VTAB benchmark [83] and "VTAB-1K" is the average over all 19 datasets of the VTAB-1K benchmark. ADE20K reports the mean intersection over union (mIoU) of a semantic segmentation probe. MIM-Refiner learns general features that can easily be transferred to various datasets and tasks. Table 15 confirms this finding on additional models and Appendix E.10 shows individual VTAB performances for VTAB-6 probing and VTAB-1K fine-tuning.

		iNat18 Fine-tuning			**Linear Probe**			**VTAB-1K**
ViT	Method	1-shot	5-shot	10-shot	iNat18	VTAB-6	ADE20K	Fine-tuning
L/16	MAE	7.1	51.6	68.9	42.8	83.0	33.6	73.7
	iBOT	15.8	51.5	65.5	56.0	87.6	35.6	70.8
	Mugs	**19.5**	53.2	66.9	**61.5**	87.9	34.8	68.0
	MAE-Ref.	19.0	**58.0**	**71.7**	60.6	**88.5**	**37.3**	**75.2**
H/14	MAE	6.5	53.3	71.7	43.0	83.2	35.5	72.7
	MAE-CT	16.5	60.1	74.7	62.8	88.8	37.6	75.7
	MAE-Ref.	**20.9**	**62.4**	**75.4**	**64.6**	**89.3**	**39.4**	**75.9**
2B/14	MAE	10.0	53.7	72.2	51.0	85.4	37.3	74.1
	MAE-Ref.	**22.5**	**63.5**	**76.5**	**69.6**	**89.8**	**40.3**	**75.6**

Table 6: Full fine-tuning using 100% of the labels. MIM-Refiner consistently improves performance slightly even though ID methods typically perform worse than MIM models on this benchmark. Appendix Table 18 confirms this pattern on additional MIM models. "Robustness" shows the average performance of the trained IN-1K classifier on robustness datasets (individual results in Table 19).

	ViT-L/16				**ViT-H/14**		
Model	IN-1K	Robustness	iNat18	ADE20K	IN-1K	Robustness	iNat18
D2V2	86.6	60.2	81.0	**54.4**	86.6	63.2	79.6
D2V2-Ref.	**86.7**	**60.5**	**81.6**	**54.4**	**86.8**	**64.1**	**79.8**
dBOT [50]	85.8	**55.3**	81.9	53.1	**87.1**	63.7	84.1
dBOT-Ref.	**85.9**	**55.3**	**82.1**	**53.3**	**87.1**	**64.0**	**84.5**
Mugs [87]	85.2	46.4	76.9	50.2	-	-	

C.5 Fine-tuning with Large Amounts of Labels

MIM models typically outperform ID methods when given enough labels to fine-tune the model. As our refinement process employs an ID objective, we investigate whether MIM-Refiner involuntarily degrades performance given an abundance of labels. To this end, we fine-tune MIM models and their refined version on ImageNet-1K [20], iNat18 [36] and ADE20K [85] using a classification/UperNet [78] head. Table 6 shows a small but consistent improvent of MIM-Refiner models.

D Limitations

One limitation of MIM-Refiner is that it requires batch normalization [40] layers in the ID head. Without them, performance decreases significantly. As we do not change anything in the MIM pre-training, we hypothesize that feature statistics after MIM pre-training are not suited for an ID task and therefore require per-feature normalization. The batch normalization layers significantly decrease scalability to distributed hardware setups as each layer requires a synchronization of batch statistics.

MIM-Refiner addresses a common issue with MIM models: their typically lightweight decoder often delegates part of the reconstruction to the encoder, resulting in subpar representations for the later encoder blocks in downstream tasks. Alternatively, one could simply argue for a larger decoder. However, a larger decoder increases computational costs since the decoder typically operates on the full sequence length. Additionally, the direction of a larger decoder was explored to a certain extent in the original MAE paper [30], where larger decoders performed worse in fine-tuning and linear probing. Successor models such as CrossMAE perform well with a deeper decoder but still show decreasing representation quality in later layers, as shown in Appendix E.4.

During early development, we tried various ways to propagate the intermediate representation towards the end. While we found that a simple ensemble of contrastive heads attached to later blocks works very well, there might be even better ways to leverage the rich intermediate MIM representations. We explored the following variants in with little success: (i) completely deleting the last few blocks (ii) reinitializing the last few blocks while setting the weights/biases of the last projection in the attention/MLP to 0 which leads to the result of the previous block being propagated to the end via the residual connection (iii) gating the last few blocks via ReZero [5].

To address the limitation of MIM-Refiner requiring batch normalization layers, we explore another variant that copies the weights of the intermediate block with the highest k-NN accuracy to all subsequent blocks and sets the weights/biases of the last projection in the copied attention/MLP blocks to 0. This is similar to the above mentioned approach (ii), except that the weights of the copied blocks are not random but copied from an intermediate block. We then train the model with only a single head attached at the last block. This drastically reduces the number of batch normalization layers. Table 7 shows that such an approach can yield competitive performances on smaller models, but is outperformed by MIM-Refiner on larger ones.

Table 7: Copying the peak-representation block to subsequent blocks while setting the last attention/MLP projection weights/biases to 0 can improve scalability to even larger distributed setups due to requiring less batch normalization [40] layers. This approach ("Copy Blocks") is competitive to an ensemble of ID heads ("MIM-Refiner") on smaller models but is worse on larger models.

k-NN	MAE L/16	MAE H/14
Copy Blocks	**81.5**	81.8
MIM-Refiner	**81.5**	**82.3**

Another approach to improve scalability to larger distributed systems is to only aggregate batch statistics within a node. This avoids costly inter-node communication and instead only requires intra-node connections which is typically much faster.

As MIM-Refiner is quite computationally efficient even with the batchnorm synchronization limitation, we do not explore these approaches further.

E Extended Results

E.1 Extended Representation Quality Comparison

We compare linear probing performance and runtime against non-publicly available models using the reported values from their respective paper in Figure 5.

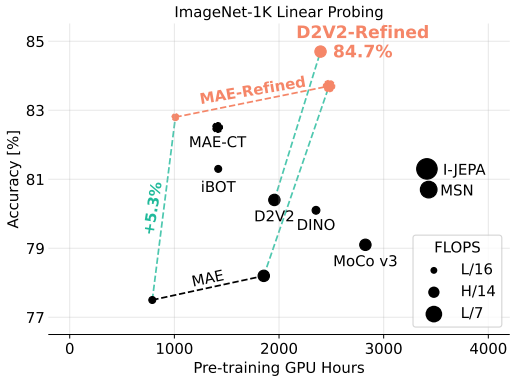

Figure 5: Representation quality of SSL methods evaluated via linear probing. MIM-Refiner advances state-of-the-art among models pre-trained on ImageNet-1K in low- and high-compute regimes.

E.2 Where to Attach ID Heads?

Table 8 ablates different choices of where to attach ID heads on a D2V2 pre-trained ViT-L/16 and ViT-H/14. On ViT-L/16, there is almost no difference of where to attach the ID heads in the last third of blocks. We tried to transfer this insight to ViT-H/14 where the default setting of attaching ID heads to all later blocks performs better. We therefore use the default setting of attaching ID heads to the last 8 blocks (ViT-L and ViT-2B) or the last 12 blocks (ViT-H).

Table 8: Spacing heads out more across the later ViT blocks can achieve comparable performances for ViT-L/16 but does not generalize to ViT-H/14. The default setting of attaching ID heads to all later blocks generalizes well across model scales.

Block Indices	k-NN
20,24	80.9
16,20,24	**81.1**
15,18,21,24	**81.1**
18,20,22,24	81.0
17-24	81.0

(a) ViT-L/16

Block Indices	k-NN
22,24,26,28,30,32	82.0
16,18,20,22,24,26,28,30,32	82.1
20-32	**82.3**

(b) ViT-H/14

E.3 Freezing Early Blocks

Freezing early blocks as a form of regularization to preserve MIM features (similar to related works [47, 41]) is not necessary. Note that we still use a layer-wise learning rate decay [17].

Table 9: Freezing early blocks is not necessary and slightly decreases performance. Ablation conducted with D2V2-L/16. We freeze the first 6 layers to refine MAE-2B to save memory/compute.

#Frozen	k-NN
0	**81.0**
6	80.9
12	80.6

E.4 Intermediate Representation Analysis of Additional MIM Methods

We visualize the k-NN accuracies of various MIM models in Figure 6 where all of them show the pattern that the representation quality of larger models degrades towards the end of the encoder.

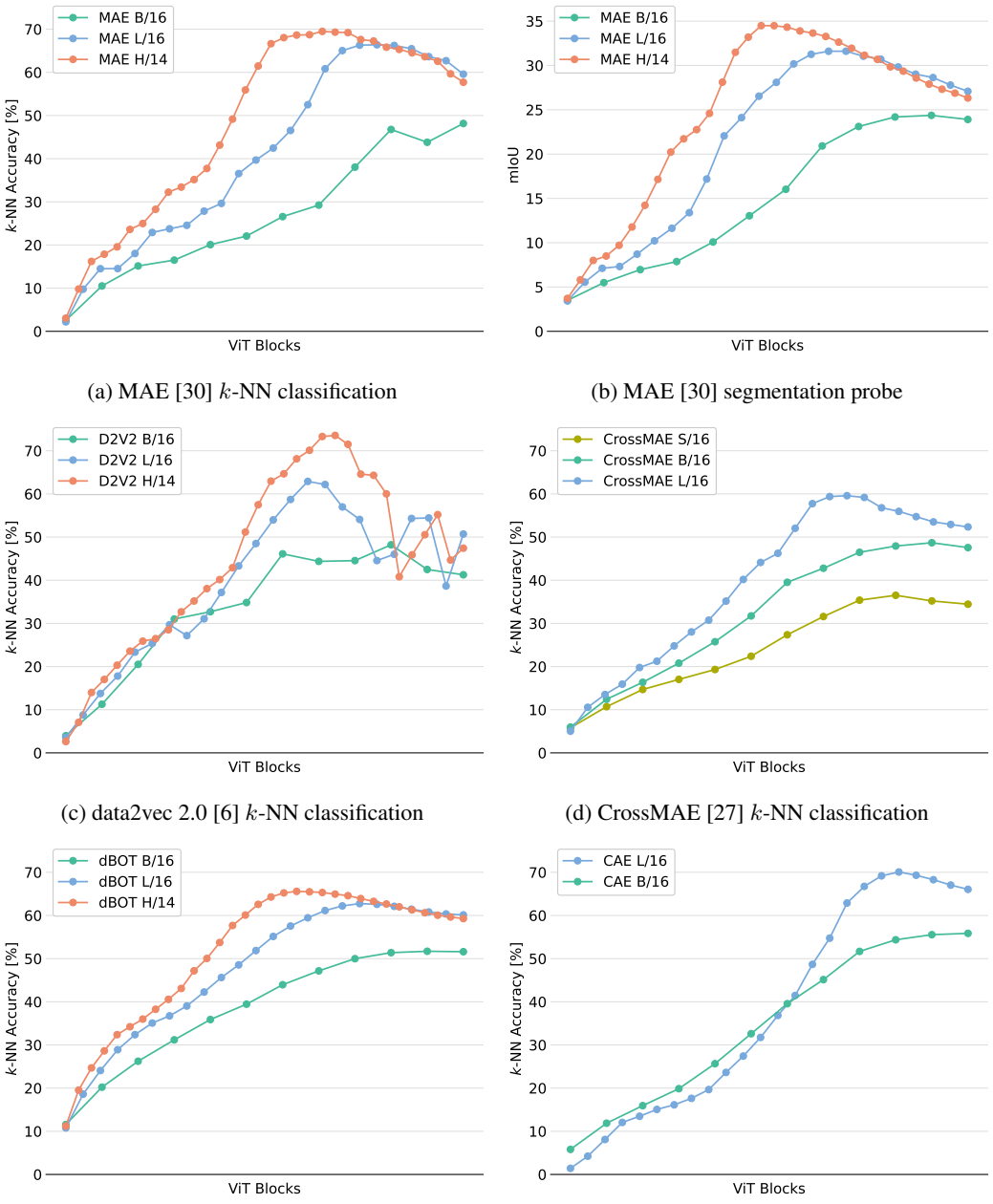

(a) MAE [30] k-NN classification

(b) MAE [30] segmentation probe

(c) data2vec 2.0 [6] k-NN classification

(d) CrossMAE [27] k-NN classification

(e) dBOT [50] k-NN classification

(f) CAE [15] k-NN classification

Figure 6: Intermediate representation analysis of various MIM models. As models get bigger, the k-NN accuracy degrades more towards the end of the encoder, especially for L/16 and H/14 models. This pattern is consistent over various MIM models and across tasks. k-NN accuracy is calculated on ImageNet-1K [20]. (b) shows the mIoU of linear segmentation probes on ADE20K [85].

E.5 Low-shot Classification Without Color Augmentations

MAE-CT [47] showed that omitting color augmentations can lead to performance gains for low-shot classification, especially on larger models. We therefore train our ViT-H/14 models also without color augmentations. We use the same hyperparameters as with color augmentations (see Table 23) except that we disable color augmentations (i.e. we train with only crop & flip augmentations) and half the training duration. Table 10 confirms the findings of [47] as omitting color augmentations also improves low-shot performance of MIM-Refiner.

Table 10: ImageNet-1K low-shot and feature evaluations of a D2V2-Refined-H/14 with and without color augmentations. Omitting color augmentations improves ImageNet-1K low-shot performance.

		Low-shot Evaluation					**Feature Eval**	
Model	Color/blur	1-shot	2-shot	5-shot	1%	10%	Probe	k-NN
D2V2-Refined	✗	**64.7**	**72.0**	**75.9**	**79.1**	**83.5**	84.1	82.1
	✓	64.2	71.3	75.5	78.1	**83.5**	**84.7**	**82.3**

E.6 Extended ImageNet-1K Low-shot and Feature Evaluations

Table 11: Extending Table 3 with additional MIM-Refiner models and more SSL models. The last row-group compares the best MIM-Refiner model to models with longer sequence length (MSN-L/7) and models that were pre-trained on more data. Parentheses show pre-training dataset size. MIM-Refiner consistently improves MIM models, outperforms other SSL models with the same pre-training data and even outperforms DINOv2-g/14 in some settings.

		Low-shot Evaluation					**Feature Eval**	
ViT	Method	1-shot	2-shot	5-shot	1%	10%	Probe	k-NN
L/16	CrossMAE [27]	16.8	34.0	52.4	63.2	77.7	74.4	53.4
	MAE [30]	14.3	34.9	56.9	67.7	79.3	77.5	60.6
	dBOT [50]	28.0	46.9	62.4	70.0	80.2	77.8	61.3
	D2V2 [6]	24.1	58.8	72.1	75.1	81.5	78.2	51.8
	CAE [15]	28.1	56.5	68.4	71.4	79.5	80.0	66.9
	iBOT [86]	48.5	58.2	66.5	73.3	79.0	81.1	78.0
	Mugs [87]	52.9	62.3	69.4	76.2	80.3	82.1	80.4
	CrossMAE-Refined	50.3	60.9	68.2	71.7	79.3	81.8	79.9
	MAE-Refined	57.8	66.3	72.0	76.1	81.2	82.8	**81.5**
	dBOT-Refined	57.4	66.0	71.7	76.6	81.6	83.3	81.3
	D2V2-Refined	**61.7**	**69.6**	**73.9**	**78.1**	**82.1**	**83.5**	81.0
H/14	MAE [30]	7.2	14.1	40.2	72.8	81.2	78.2	58.1
	dBOT [50]	23.9	45.0	63.0	73.0	82.1	79.0	60.0
	D2V2 [6]	21.6	60.8	74.2	77.6	83.3	80.4	48.0
	I-JEPA [3]	35.1	47.9	59.9	73.3	79.5	79.3	71.6
	MAE-CT [47]	49.4	59.6	67.4	74.4	81.7	82.3	79.1
	MAE-Refined	59.5	68.5	73.8	77.4	82.1	83.7	**82.3**
	dBOT-Refined	59.2	67.6	72.9	77.3	82.5	84.0	82.0
	D2V2-Refined	**64.2**	**71.3**	**75.5**	**78.1**	**83.5**	**84.7**	**82.3**
2B/14	MAE [30, 65]	17.8	29.1	62.9	73.6	82.0	79.7	67.1
	MAE-Refined	**58.2**	**68.6**	**74.8**	**78.7**	**82.5**	**84.5**	**83.2**
L/16	iBOT [86] (14M)	37.4	49.9	61.9	70.9	80.3	82.7	72.9
L/7	MSN [2] (1.3M)	57.1	66.4	72.1	75.1	-	80.7	-
H/14	D2V2-Refined (1.3M)	**64.2**	**71.3**	**75.5**	78.1	83.5	84.7	82.3
g/14	DINOv2 [56] (142M)	60.5	68.3	74.4	**79.1**	**83.8**	**86.5**	**83.5**

E.7 Extended ImageNet-1K Cluster Evaluations

Table 12 extends the main paper results (Table 4) with additional models. Table 13 shows the average clustering results of the 100 mini-batch k-means runs as described in Section C.3. We see that MIM-Refiner has also better average performance than competitor methods.

Table 12: Best k-means cluster performance and class separation on ImageNet of recent SSL models. This table extends Table 4 from the main paper with additional comparison and refined models.

		Cluster Performance				**Class Separation**	
ViT	Method	ACC	NMI	AMI	ARI	SIL (↑)	DBS (↓)
L/16	MAE [30]	18.5	55.2	29.1	6.9	-5.9	5.0
	D2V2 [6]	10.5	45.1	19.5	2.5	-9.1	6.4
	iBOT [86]	52.2	80.5	67.0	33.4	13.3	3.5
	Mugs [87]	54.3	78.6	65.5	22.4	14.9	3.3
	MAE-Refined	61.8	84.0	72.6	**40.7**	21.4	2.9
	D2V2-Refined	**67.4**	**86.3**	**76.2**	40.5	**37.1**	**2.2**
H/14	MAE [30]	14.3	50.2	24.2	4.3	-7.8	5.2
	D2V2 [6]	9.9	45.8	18.0	2.6	-10.8	6.5
	MAE-Refined	64.6	85.3	74.6	**45.5**	21.0	2.9
	D2V2-Refined	**67.3**	**87.2**	**77.9**	42.2	**34.5**	**2.3**
2B/14	MAE [30]	19.9	54.1	33.1	6.2	-3.6	4.8
	MAE-Refined	**63.0**	**85.0**	**74.4**	**44.0**	**14.0**	**3.2**
g/14	DINOv2 [56]	47.7	76.3	63.6	5.1	30.4	2.8

Table 13: Average k-means cluster performance on ImageNet of recent SSL models. MIM-Refiner drastically improves performance of unrefined models and outperforms competitors.

		Cluster Performance			
ViT	Method	ACC	NMI	AMI	ARI
L/16	MAE [30]	17.9	54.5	28.9	6.5
	D2V2 [6]	10.2	44.5	19.3	2.3
	iBOT [86]	50.5	80.0	66.6	31.6
	Mugs [87]	50.7	77.4	64.4	18.1
	MAE-Refined	**60.6**	83.5	71.9	**35.0**
	D2V2-Refined	**60.6**	**83.9**	**72.9**	30.0
H/14	MAE [30]	13.8	49.8	24.4	4.2
	D2V2 [6]	9.7	45.2	18.1	2.5
	MAE-Refined	**63.2**	**84.7**	74.0	**40.1**
	D2V2-Refined	60.4	84.5	**74.3**	28.4
2B/14	MAE [30, 65]	19.2	53.5	32.9	5.7
	MAE-Refined	**59.4**	**84.0**	**73.4**	**38.0**
g/14	DINOv2 [56]	46.8	75.6	62.7	3.5

Figure 7 shows an additional analysis on the cluster structure in each of the blocks for the refined and unrefined MAE and D2V2 models with ViT-H/14 on ImageNet-1K. Corresponding to the k-NN accuracy analysis in Figure 3b, we see that MAE and D2V2 have a higher cluster accuracy (ACC) in the intermediate blocks than in the last block. MIM-Refiner turns this behaviour around and causes a steep increase of ACC starting from the intermediate block and continuing to almost 70% in the last layer. The silhouette score (SIL) confirms this as well. The early blocks allow no separation of the ground truth ImageNet-1K classes leading to negative SIL values, whereas later blocks of the refined models increase separation by 30-50% compared to unrefined counterparts. Interestingly, MAE-Refined is not plateauing in SIL and ACC compared to D2V2-Refined, pointing to potential room for improvement in MAE refinement by using additional ID heads at earlier layers. The bottom part of Figure 7 measures the pairwise cluster label similarity between subsequent blocks in terms of normalized mutual information (NMI) [45] as $(\mathrm{NMI}(y_i, y_{i+1})) \cdot 100$, where y_i are the k-means

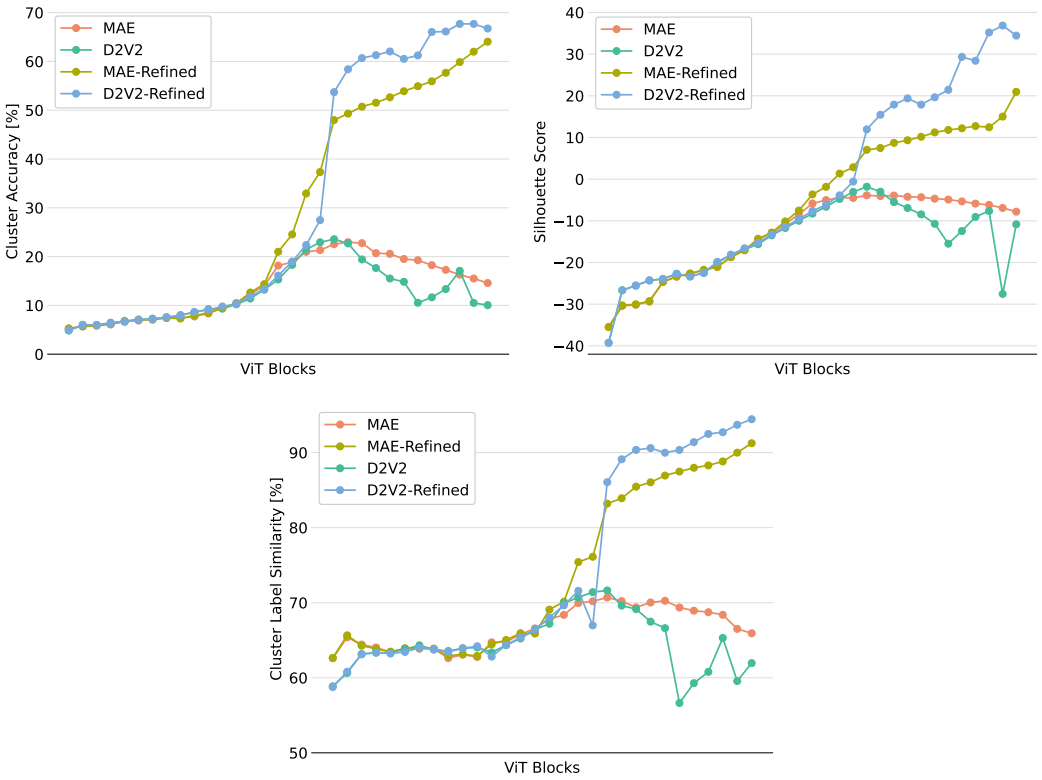

Figure 7: Block-wise cluster analysis for refined and unrefined MAE and D2V2 (H/14). **Upper Left**: Cluster accuracy w.r.t. lowest k-means loss per block. **Upper Right**: Silhouette score w.r.t. ground truth ImageNet-1K classes. **Bottom**: Pairwise cluster label similarity between subsequent blocks (details in Section E.7).

cluster labels at block i. The low cluster label similarity in the early blocks for all models indicates that the found cluster labels focus on different clusterings. The later blocks of MIM-Refined models have high alignment with similarities of more than 90%. The higher ACC w.r.t. the ground truth ImageNet-1K classes in the later blocks indicates that they focus more on object-centric features. This is in contrast to the overall lower cluster label similarity in unrefined models, which focus on different cluster structures in each block.

E.8 Multi-model Clustering Evaluations

We evaluate unsupervised cluster accuracy of MIM-Refiner in combination with other foundation models using the TURTLE [28] framework. The results in Table 14 show that MIM-Refiner learns features that are complementary to features learned from foundation models. Combining multiple MIM-Refiner models boosts unsupervised classification accuracy of individual models surpassing the best k-means accuracy of D2V2-Ref.-H/14 (67.3%). TURTLE with the feature spaces of MAE-Ref., dBOT-Ref. and D2V2-Ref improves the state-of-the-art of unsupervised classification accuracy using only ImageNet-1K for pre-training to 71.6%. When additionally including foundation models that were pre-trained on web-scale data, MIM-Refiner consistently improves performance. MAE-Refined in combination with DINOv2 [56], CLIP [61] and SWAG [66] sets a new state-of-the-art of 76.8%.

We conduct this study by implementing MIM-Refiner models into the official implementation of TURTLE[1] and train with the recommended default settings. We do not tune any hyperparameters.

[1] https://github.com/mlbio-epfl/turtle

Table 14: Unsupervised classification evaluation using the TURTLE [28] framework. MIM-Refiner models synergize well with foundation models such as DINOv2 [56], CLIP [61] and SWAG [66]. MIM-Refiner in combination with TURTLE [28] sets a new state-of-the-art in ImageNet-1K unsupervised classification without additional data (71.6%) and with additional data (76.8%). Model sizes are H/14 for MIM-Refiner and SWAG [66], g/14 for DINOv2 [56] and L/14 for CLIP [61].

ImageNet-1K pre-training			**Web-scale pre-training**			
MAE-Ref.	dBOT-Ref.	D2V2-Ref.	DINOv2	CLIP	SWAG	ACC
MIM-Refiner only						
✗	✓	✓	✗	✗	✗	61.7
✓	✗	✓	✗	✗	✗	62.2
✓	✓	✗	✗	✗	✗	70.4
✓	✓	✓	✗	✗	✗	**71.6**
MIM-Refiner + DINOv2						
✗	✗	✗	✓	✗	✗	68.5
✗	✗	✓	✓	✗	✗	58.3
✗	✓	✗	✓	✗	✗	**74.0**
✓	✗	✗	✓	✗	✗	73.7
MIM-Refiner + DINOv2 + CLIP						
✗	✗	✗	✓	✓	✗	72.9
✗	✗	✓	✓	✓	✗	69.4
✗	✓	✗	✓	✓	✗	**75.0**
✓	✗	✗	✓	✓	✗	**75.0**
MIM-Refiner + DINOv2 + CLIP + SWAG						
✗	✗	✗	✓	✓	✓	74.8
✗	✗	✓	✓	✓	✓	74.9
✗	✓	✗	✓	✓	✓	76.4
✓	✗	✗	✓	✓	✓	**76.8**

E.9 Extended Transfer Learning Results

Table 15 extends Table 5 with additional results and comparison to more SSL models.

Table 15: Extending Table 5 with additional MIM-Refiner models and additional SSL models. MIM-Refiner learns general features that can easily be transferred to various datasets and tasks.

		iNat18 Fine-tuning			**Linear Probe**		
ViT	Method	1-shot	5-shot	10-shot	iNat18	VTAB-6	ADE20K
L/16	CrossMAE [27]	5.4	45.6	63.7	39.8	81.2	30.9
	MAE [30]	7.1	51.6	68.9	42.8	83.0	33.6
	dBOT [50]	7.1	53.1	71.2	44.6	83.4	34.1
	D2V2 [6]	5.5	53.1	70.6	39.4	81.5	38.8
	CAE [15]	7.4	54.5	71.2	46.4	84.8	36.5
	iBOT [86]	15.8	51.5	65.5	56.0	87.6	35.6
	Mugs [87]	**19.5**	53.2	66.9	61.5	87.9	34.8
	CrossMAE-Ref	18.0	52.9	67.8	60.5	88.3	34.3
	MAE-Ref	19.0	58.0	71.7	60.6	**88.5**	37.3
	dBOT-Ref	18.3	**58.8**	**73.0**	**61.7**	**88.5**	38.4
	D2V2-Refined	15.2	56.3	71.8	52.0	85.9	**41.0**
H/14	MAE [30]	6.5	53.3	71.7	43.0	83.2	35.5
	dBOT [50]	6.8	53.1	73.2	46.2	84.6	36.1
	D2V2 [6]	5.9	55.7	73.4	41.7	83.1	42.4
	MAE-CT [47]	16.5	60.1	74.7	62.8	88.8	37.6
	MAE-Ref	**20.9**	**62.4**	75.4	64.6	89.3	39.4
	dBOT-Ref	20.0	60.9	**75.8**	**65.8**	**89.5**	37.6
	D2V2-Refined	16.1	59.2	74.8	54.4	87.1	**43.7**
2B/14	MAE [65]	10.0	53.7	72.2	51.0	85.4	37.3
	MAE-Ref	**22.5**	**63.5**	**76.5**	**69.6**	**89.8**	**40.3**
L/7	MSN [2]	17.0	38.0	48.1	-	-	-

E.10 VTAB Individual Dataset Results

We show the individual accuracies for each VTAB [83] dataset from Table 5 of the main paper. Table 16 shows linear probing results on VTAB and Table 17 shows fine-tuning results on VTAB-1K. We use only six datasets for linear probing, as the other datasets are quite different to the ImageNet-1K images seen during training and therefore benefit heavily from fine-tuning which makes them more suited for evaluation via fine-tuning instead of linear probing.

Table 16: Linear probing accuracy on six VTAB [83] datasets from the "Natural" category: Caltech101 [26], CIFAR100 [44], DTD [16], Flowers102 [55], Pets [57] and Sun397 [77].

		VTAB Dataset						
ViT	Method	CF100	CT101	DTD	FL102	Pets	Sun397	Average
L/16	CrossMAE	81.4	88.8	75.6	84.2	84.1	72.7	81.2
	MAE	80.0	91.8	75.6	86.3	89.6	74.7	83.0
	dBOT	84.3	91.3	75.7	88.0	86.0	75.1	83.4
	D2V2	85.0	89.8	74.0	84.9	80.7	74.6	81.5
	CAE	87.0	92.3	76.1	88.4	89.2	75.9	84.8
	iBOT	89.3	91.3	78.1	95.8	93.7	77.1	87.6
	Mugs	89.5	90.5	78.0	**96.8**	95.3	77.2	87.9
	CrossMAE-Ref	88.7	**93.5**	**79.0**	95.7	95.2	78.1	88.3
	MAE-Ref	89.1	91.9	**79.0**	96.2	**95.8**	78.8	**88.5**
	dBOT-Ref	**90.4**	91.3	78.6	95.9	95.5	**79.2**	**88.5**
	D2V2-Ref	88.9	88.8	73.9	92.1	94.7	77.1	85.9
H/14	MAE	81.0	90.3	76.9	85.9	89.5	75.3	83.2
	dBOT	85.5	91.7	77.7	88.1	88.2	76.3	84.6
	D2V2	87.1	91.4	77.4	85.9	79.9	76.9	83.1
	I-JEPA	87.1	92.7	72.5	90.4	92.4	74.9	85.0
	MAE-CT	87.7	**93.9**	80.1	97.0	95.0	79.2	88.8
	MAE-Ref	90.1	92.0	80.4	**97.5**	96.0	79.8	89.3
	dBOT-Ref	**91.7**	92.1	**80.6**	96.7	**96.1**	**80.1**	**89.5**
	D2V2-Ref	90.4	89.0	75.9	93.3	95.6	78.4	87.1
2B/14	MAE	82.5	92.0	78.2	90.5	91.8	77.1	85.4
	MAE-Ref	**90.8**	**92.6**	**81.1**	**97.7**	**96.5**	**80.3**	**89.8**

Table 17: Fine-tuning accuracy of all 19 VTAB-1K [83] datasets (averages are reported in Table 5). Row-groups correspond to ViT-L/16, ViT-H/14 and ViT-2B/14 models respectively.

	Natural							Specialized				Structured							
Method	CF100	CT101	DTD	FL102	Pets	SVHN	Sun397	Camelyon	EuroSAT	Resisc45	Retinopathy	Clevr-Count	Clevr-Dist	DMLab	KITTI-Dist	dSpri-Loc	dSpr-Ori	sNORB-Azi	sNORB-Ele
MAE	50.3	90.1	68.0	90.8	92.7	**92.2**	35.1	**85.5**	93.2	81.7	72.7	**93.2**	63.9	55.8	**84.5**	**93.9**	58.6	**46.1**	**51.9**
iBOT	68.3	**91.5**	**71.5**	95.8	91.8	80.1	47.6	85.4	93.4	86.6	74.5	79.9	61.7	52.3	80.2	74.5	47.2	27.5	35.4
Mugs	**69.4**	89.2	71.4	95.4	92.9	78.1	47.6	85.2	94.0	86.2	**74.7**	75.1	53.0	51.1	77.9	46.8	45.5	26.3	32.6
MAE-Ref	62.2	90.6	**71.5**	**97.2**	**93.7**	91.7	**49.1**	85.3	**94.8**	**86.8**	73.4	92.5	**64.3**	**57.4**	84.3	88.4	**60.5**	39.0	46.5
MAE	44.3	88.3	67.8	90.8	90.8	**91.1**	30.4	85.9	94.0	81.3	73.9	92.7	63.6	54.0	84.9	92.2	62.8	37.1	**55.2**
MAE-CT	58.5	**93.2**	72.3	97.5	93.4	90.7	48.3	85.9	94.4	86.1	75.0	**93.0**	**64.9**	**58.3**	83.6	91.9	**63.8**	**38.0**	48.7
MAE-Ref	**62.3**	91.3	**73.1**	**97.9**	**93.9**	89.5	**49.7**	**86.8**	**94.9**	**87.7**	**75.1**	92.9	63.3	57.5	**85.9**	**93.5**	62.2	36.0	49.3
MAE	44.7	90.4	70.0	91.8	92.4	**92.3**	33.8	85.9	94.2	82.6	**74.2**	92.4	63.9	55.5	**85.5**	**94.6**	61.1	**44.9**	**57.9**
MAE-Ref	**61.8**	**91.0**	**73.9**	**97.5**	**94.5**	91.3	**49.1**	**86.6**	**94.7**	**87.0**	73.8	**92.6**	**64.7**	**58.8**	85.3	93.5	**61.2**	37.9	40.9

E.11 Extended Comparison of Fine-tuning on ImageNet-1K and iNat18

Table 18 extends Table 6 with additional MIM models. MIM-Refiner consistently improves also on fine-tuning with an abundance of labels.

Table 18: Full fine-tuning using 100% of the labels. MIM-Refiner consistently improves performance slightly even though ID methods typically perform worse than MIM models on this benchmark. This table extends Table 6 from the main paper with additional MIM models and SSL models.

	ViT-L/16		**ViT-H/14**	
Model	ImageNet-1K	iNat18	ImageNet-1K	iNat18
MAE	**85.7**	80.7	86.7	82.7
MAE-CT [47]	85.4	**80.9**	86.8	82.9
MAE-Refined	85.6	**80.9**	**86.9**	**83.3**
CrossMAE	84.9	77.7	-	-
CrossMAE-Refined	**85.1**	**78.4**	-	-
D2V2	86.6	81.0	86.6	79.6
D2V2-Refined	**86.7**	**81.6**	**86.8**	**79.8**
dBOT	85.8	81.9	**87.1**	84.1
dBOT-Refined	**85.9**	**82.1**	**87.1**	**84.5**
iBOT	84.8	76.9	-	-
Mugs	85.2	76.9	-	-
I-JEPA	-	-	84.9	75.9

Table 19: Robustness and domain generalization evaluation on ImageNet-C(orruption) [33] ImageNet-A(dversarial) [35], ImageNet-R(endition) [32] and ImageNet-Sketch [73]. For ImageNet-C we report the mean corruption error [33]. MIM-Refiner consistently improves robustness, particularly on larger models. Table 6 reports the average accuracy of IN-A, IN-R and IN-Sketch.

ViT	Method	IN-C (↓)	IN-A (↑)	IN-R (↑)	Sketch (↑)	Validation (↑)
L/16	CrossMAE	41.0	51.8	**57.1**	42.0	84.9
	CrossMAE-Ref.	**40.7**	**52.1**	57.0	**42.1**	**85.1**
L/16	MAE	39.2	56.2	60.0	45.6	**85.7**
	MAE-Ref.	**39.0**	**57.0**	**60.1**	**45.9**	85.6
L/16	D2V2	34.0	66.1	**64.4**	50.0	86.6
	D2V2-Ref.	**33.5**	**67.2**	64.3	**50.1**	**86.7**
L/16	dBOT	**36.1**	60.0	**60.5**	**45.5**	85.8
	dBOT-Ref.	**36.1**	**60.3**	60.4	45.3	**85.9**
L/16	iBOT	37.8	47.6	53.7	41.9	84.5
	Mugs	39.9	47.8	52.0	39.3	84.6
H/14	MAE	34.6	67.8	64.1	48.9	86.7
	MAE-Ref.	**34.3**	**68.0**	**65.1**	**49.7**	**86.9**
H/14	D2V2	30.7	72.9	65.7	51.0	86.6
	D2V2-Ref.	**30.2**	**74.1**	**66.1**	**52.1**	**86.8**
H/14	dBOT	**31.8**	71.1	**68.1**	**51.8**	**87.1**
	dBOT-Ref.	**31.8**	**72.3**	68.0	**51.8**	**87.1**
H/14	I-JEPA	37.4	51.7	57.4	43.7	81.7
2B/14	MAE	32.6	68.4	65.4	50.0	86.7
	MAE-Ref.	**32.2**	**68.9**	**66.2**	**50.5**	**86.8**

E.12 Fine-tuning ViT-2B Models

Table 20 shows results for fine-tuning ViT-2B models.

Table 20: Fine-tuning ViT-2B models using 100% of the labels. As fine-tuning these models is expensive, we freeze the first 6 of the 24 blocks to save memory and compute.

	ViT-2B/14	
Model	ImageNet-1K	iNat18
MAE	86.7	82.2
MAE-Refined	**86.9**	**83.2**

E.13 Impact of Multi-Crop Augmentation

Multi-crop augmentation [10] has been shown to greatly improve the performance of ID methods [10, 11, 86, 87] and also improves MIM-Refiner significantly, where the k-NN accuracy of a D2V2-Refined L/16 drops by 2.6% when omitting multi-crop augmentations. When comparing to drops of other models, this is a relatively small drop. For example, the performance of DINO B/16 drops by 7.2% and iBOT B/16 drops by 5.6% when omitting multi-crop augmentations (see Table 10 in [86]).

E.14 High-dimensional k-NN

The linear probing protocol of DINOv2 [56] includes the possibility to concatenate features of the last 4 blocks as input to the linear probe. We find that this outperforms using only the features of the last block in most cases. As the best linear probe uses features from the last 4 blocks and the fact that the k-NN and linear probing metrics are typically correlated [56], we report the k-NN accuracy using only the features of the last block in Table 3 to use the last 4 blocks for one metric and only the last block for the other. In Table 21 we investigate using the concatenation of features from the last 4 blocks for a k-NN classifier. Most models benefit from using more features, especially MIM models.

Table 21: ImageNet-1K k-NN accuracy at 224x224 resolution of the [CLS] token of the last block or the concatenation of the [CLS] tokens of the last 4 blocks.

		#Blocks		
ViT	Method	1	4	Delta
L/16	MAE	60.6	63.3	+2.7
	D2V2	51.8	52.9	+1.1
	iBOT	78.0	78.9	+0.9
	Mugs	80.4	80.1	-0.3
	MAE-Refined	**81.5**	81.5	0.0
	D2V2-Refined	81.0	**81.7**	+0.7
H/14	MAE	58.1	61.4	+3.3
	D2V2	48.0	52.2	+4.2
	I-JEPA	71.6	72.3	+0.7
	MAE-CT	79.1	78.6	-0.5
	MAE-Refined	**82.3**	82.5	+0.2
	D2V2-Refined	**82.3**	**83.4**	+1.1
g/14	DINOv2	83.0	83.9	+0.9

E.15 MIM-Refiner on Smaller Models

MIM-Refiner builds on pre-trained MIM models which excel at larger scales (ViT-L and upwards), we mainly focus on large-scale models in our paper. However, MIM-Refiner also improves MIM models on smaller scales (ViT-B). Additionally, combinations of MIM and ID methods have been explored in various works [38, 74, 82]. However, as these methods introduce significant runtime overhead over MIM models, they mainly focus on smaller models (ViT-L and smaller) where the pre-trained

models are also often not published, which makes a comprehensive comparison against these models impossible. Nevertheless, we show that MIM-Refiner is complementary to these methods by refining a Contrastive MAE [38] ViT-B/16 model with MIM-Refiner. Table 22 shows that MIM-Refiner also significantly improves representation quality on smaller models.

Table 22: MIM-Refiner also significantly improves ViT-B models. Methods that improve MIM by incorporating ID already during pre-training are orthogonal to MIM-Refiner where the refinement process also significantly improves representation quality of these models.

ViT-B/16	k-NN	5-shot	2-shot	1-shot
MAE	51.1	43.1	27.1	14.0
MAE-Refined	**76.6**	**64.5**	**58.6**	**50.0**
CMAE [38]	76.7	43.3	31.2	21.7
CMAE-Refined	**78.5**	**70.1**	**65.7**	**57.9**

F Implementation Details

F.1 Evaluations

To avoid slight performance differences due to minor implementation details or version changes and facilitate a fair comparison between models, we run all evaluations on our own in accordance with the suggested hyperparameters of the respecitve methods.

F.2 Hardware

All models are pre-trained on multiple nodes of 4xA100-64GB GPUs where ViT-L uses 4 nodes (i.e. 16 GPUs), ViT-H 8 nodes of 4xA100 (i.e. 32 GPUs) and ViT-2B uses 16 nodes (i.e. 64 GPUs). For evaluations, we use a mix of 4xA100-64GB nodes, 8xA100-40GB nodes and various smaller nodes that vary in number of GPUs. We estimate the total number of A100 GPU-hours used for this project to be 40K hours. This estimate includes everything from initial exploration, method development, analysis and evaluations.

F.3 Vision Transformer

The architecture of our models follows the ones from the respective MIM model that is refined. That is a pre-norm architecture for MAE [30] and a post-norm architecture for data2vec 2.0 [6]. We attach the ID heads to the [CLS] tokens and also use the [CLS] token for evaluation.

We download the official checkpoints from the respective MIM works. Note that the official CrossMAE model is pre-trained for less epochs than all other MIM models. For dBOT we use the models where a teacher of the same size is used (i.e. dBOT-L used MAE-L as teacher and dBOT-H used MAE-H as teacher).

F.4 ID Head Architecture

We use a three layer MLP with hidden dimension 2048 as projector and a two layer MLP with hidden dimension 4096 as predictor. Each linear projection is followed by a GELU [34] and a batchnorm [40] layer. For the last linear projection in projector and predictor, no GELU is used.

F.5 Refinement Hyperparameters

Hyperparameters for the refinement stage are listed in Table 23. Following MAE-CT [47], we initialize all ID heads first by training them with a frozen encoder to ensure a good learning signal from the start of the refinement process. For this initialization, we use the same hyperparameters as in Table 23 except that we use 20 epochs for all models, a learning rate of 2e-4 and a top1-NN lookup. As we do not use a momentum encoder during training, we instead track an EMA of the encoder and use the EMA then for downstream tasks. As ViT-2B is very expensive to train, we freeze the first 6 blocks (for refinement and also for evaluation). As shown in Table 9 this slightly reduces performance but also reduces memory consumption and runtime.

Table 23: MIM-Refiner hyperparameters.

Parameter	Value	Parameter	Value
Epochs	30 (MAE/dBOT L/H) 20 (MAE 2B, data2vec 2.0)	NNCLR Heads	
Batch Size	1024 (L), 512 (H, 2B)	Weight Decay	1e-5
Optimizer	AdamW [42, 51]	Temperature	0.2 (L), 0.3 (H), 0.35 (2B)
Learning Rate	4e-4	topk-NN k	20
Momentum	$\beta_1 = 0.9, \beta_2 = 0.95$	NN-swap for Positives	✓
Learning Rate Schedule	Linear Warmup $\rightarrow$ Cosine Decay	NN-swap for Negatives	✗
Warmup Epochs	4	Data Augmentation	
End Learning Rate	1e-6	Color & Blur Settings	see BYOL [29]
Encoder		Global Views	2
Layer-wise LR Decay [17]	0.65	Global View Resolution	224
Freeze Blocks	0 (L/H), 6 (2B)	Global View Scale	[0.25, 1.0]
Weight Decay	0.05	Local Views	10
EMA [60]	0.9999	Local View Resolution	96 (L), 98 (H, 2B)
		Local View Scale	[0.05, 0.25]

G Evaluation Details

G.1 GPU Hours Benchmark

For benchmarking GPU hours, we follow the setup from MAE-CT [47]: we conduct a comparison by implementing all methods in a single code-base and conducting short training runs on a single A100 40GB PCIe card. These runs are executed in mixed precision training mode and with the highest possible batchsize that is a power of 2. The runtime of these benchmark runs is then extrapolated to the reported number of epochs. Benchmarks are conducted in pytorch 2.1 with CUDA 12.1. FLOPS are measured with the fvcore library[2]. For the 1-shot classification plot in Figure 2, we do not take into account that some models train on higher resolutions (e.g. DINOv2) for visual clarity.

G.2 MAE Intermediate Representation Analysis

We analyze how well the features of a ViT block are suited for reconstruction by training an MAE with a decoder attached after every ViT block. We use the same parameters as for training from scratch [30] but reduce training duration to 20 epochs, warmup to 5 epochs and the depth of all decoders to 2. The encoder remains fully frozen during training and only the decoders are trained.

For the visualization in Figure 3d, we calculate the delta from one block to the next and normalize the deltas by dividing by the maximum delta. We do this for both the k-NN accuracy and the reconstruction loss. Figure 8 shows the reconstruction loss per block and the same plot for a MAE L/16, where a similar behavior can be observed.

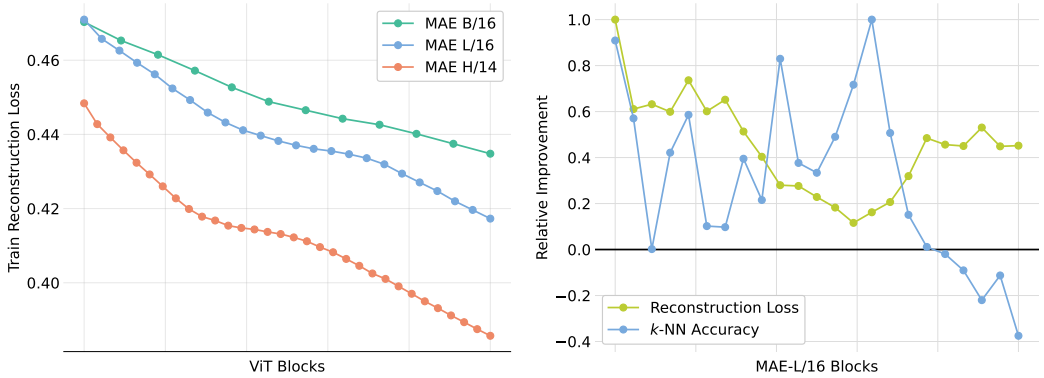

Figure 8: **Left**: Reconstruction loss per block of MAEs. **Right** Relative improvement of reconstruction loss and k-NN accuracy for a MAE L/16.

[2]https://github.com/facebookresearch/fvcore

G.3 ImageNet-1K Low-shot Evaluation Details

For the 1, 2 and 5-shot benchmarks we train a logistic regression [11, 2] using the [CLS] token after the last encoder block with the `cyanure` [52] library. As MIM models benefit from fine-tuning in this setting [2], MAE and data2vec 2.0 are fine-tuned instead. We report the average of three dataset splits from MSN [2].

In the 1% and 10% low-shot benchmark, all models are fine-tuned with hyperparameters similar to those used in related works [47, 3, 9]. As the parameters vary between 1%/10% and also between model sizes, we refer to the codebase for the exact protocols.

For a fair comparison, we conduct the low-shot evaluations of DINOv2 at 224 resolution. We study the impact of the higher resolution where we observe minimal gains at the original resolution (518x518). Note that DINOv2 first trains at 224x224 followed by a short training at 518x518 resolution.

Table 24: ImageNet-1K low-shot evaluation of DINOv2 g/14 on higher resolutions.

resolution	#patches	FLOPS [G]	1-shot	2-shot	5-shot
224x224	256	291	60.5	68.3	74.4
518x518	1369	1553	61.1	68.8	74.8

G.4 ImageNet-1K k-NN Classification Details

For k-NN classification, we follow the protocol of DINO [76, 11]. We train a soft k-NN classifier weighted by cosine similarity with $k = 10$. For MIM models, higher values for k are beneficial, so we tune this parameter for MAE and data2vec 2.0.

G.5 ImageNet-1K Linear Probing Evaluation Details

For linear probing, we use the protocol from DINOv2 [56] for publicly released models and the values from the original papers otherwise. We train for 50 epochs using SGD with momentum 0.9. As data augmentation we use `RandomResizedCrop` and `HorizontalFlip`. The DINOv2 protocol sweeps over the following hyperparameters by training multiple linear classifiers at once:

- 13 learning rates ranging from 0.0001 to 0.5
- Use the last block output or concatenate the output of the last 4 blocks
- Use the [CLS] token or the concatenation of [CLS] and [AVG] token

As the linear probes trained on the concatenation of the last 4 blocks have more features and more parameters to discriminate between classes, they tend to be the best within the sweeped parameters. Note that we evaluate the representation of the last block in isolation via k-NN classification. We investigate k-NN classification with features from the last 4 blocks in Appendix E.14.

G.6 ImageNet-1K Cluster Evaluation Details

For each considered model in the clustering experiments in Section C.3 we used the CLS token embeddings of the ImageNet validation set and preprocessed the embeddings using L2 normalization. For conducting mini-batch k-means and calculating the cluster related metrics we used the `scikit-learn` package [59], except for calculating the cluster accuracy where we used the implementation in `ClustPy` [48]. The UMAP plots in Figure 4 where generated by applying UMAP on top of the L2 normalized CLS token embeddings of the 53 food related classes of ImageNet for each model. We use the default UMAP parameters of `umap-learn` [53] for all plots (n_neighbors=15).

G.7 iNat18 Transfer Learning Evaluation Details

We report the accuracy on the validation set averaged over three seeds.

For 1-shot classification on iNat18, we use the linear probing protocol from DINOv2 [56]. We also attempted to fine-tune MIM models where some models fail to exceed random performance and therefore also use linear probing.

For 5-shot and 10-shot classification on iNat18, we fine-tune all models. The hyperparameters for fine-tuning (Table 25) are inspired by MAWS [65].

Table 25: Hyperparameters for fine-tuning on iNat18 low-shot classification.

Parameter	Value
Epochs	50
Batch size	256
Optimizer	AdamW [51, 42]
Learning rate	1e-3
Layer-wise lr decay [17]	0.75
Weight decay	0.05
Momentum	$\beta_1 = 0.9, \beta_2 = 0.999$
Learning rate schedule	linear warmup $\rightarrow$ cosine decay
Warmup epochs	5
Label smoothing [68]	0.1
Data Augmentation	
`Resize`	256
`interpolation`	bicubic
`RandomResizedCrop`	224
`scale`	[0.08, 1.0]
`interpolation`	bicubic
`RandomHorizontalFlip`	$p = 0.5$
`Normalize`	ImageNet statistics

G.8 Transfer Learning Linear Probing

For transfering the pre-trained features to iNat18, six VTAB datasets and ADE20K (Table 5) we use the DINOv2 [56] linear probing protocol as described in Appendix G.5. For ADE20K and iNat18, we reduce the hyperparameter grid to fit into 40GB GPU memory.

G.9 ADE20K Semantic Segmentation Linear Probe

Large models (such as ViT-H or ViT-2B) are expensive to train on ADE20K. Therefore, we opt for a simple light-weight evaluation protocol to compare our models on a segmentation task:

- We keep resolution at 224x224
- We freeze the encoder
- We train a linear classifier similar to DINOv2 [56] that predicts a class for each patch. The resulting low-resolution prediction is then upsampled to 224x224 resolution.
- For evaluation, we use the original resolution image and slide a 224x224 window over the image with a stride of 170 pixels and average the logits per pixel.

As intermediate representations are commonly used for semantic segmentation, we use features from the last block, the 5th last block, the 9th last block and the 13th last block. Compared to simply using the last 4 blocks, this improves performance for all compared models.

G.10 Fine-tuning on VTAB-1K

For fine-tuning models on VTAB-1K we provide the hyperparameters in Table 26. We search for the best learning rate for each dataset by fine-tuning the model 25 times (5 learning rates with 5 seeds each) on the 800 training samples and evaluating them on the 200 validation samples. With the best learning rate, we then train each model 5 times on concatenation of training and validation split, evaluate on the test split and report the average accuracy.

Table 26: Hyperparameters for fine-tuning on VTAB-1K.

Parameter	Value
Epochs	50
Batch size	64
Seeds	5
Optimizer	AdamW [51, 42]
Learning rate	1e-3, 7.5e-4, 5.0e-4, 2.5e-4, 1.0e-4
Layer-wise lr decay [17]	0.75
Weight decay	0.05
Momentum	$\beta_1 = 0.9, \beta_2 = 0.999$
Learning rate schedule	linear warmup $\rightarrow$ cosine decay
Warmup epochs	5
Data Augmentation	
`Resize`	
`interpolation`	bicubic
`size`	224x224
`Normalize`	ImageNet-1K statistics

G.11 Fine-tuning With 100% Labels

For fine-tuning with 100% of the labels (Table 6), we use the hyperparameters provided in MAE [30] for both iNat18 and ImageNet-1K (see Table 27). As D2V2 models are unstable with the default

learning rate of the MAE fine-tuning protocol, we use the highest stable learning rate out of 5e-4, 2.5e-4 and 1e-4.

For ViT-2B/14 (Table 20), we freeze the first 6 of the 24 blocks to reduce computational costs. Additionally, as the 2B models are sometimes unstable with a learning rate of 1e-3, we reduce it to 7.5e-4 or 5e-4 using the largest stable learning rate.

To fine-tune I-JEPA [3], we adjust hyperparameters to match their fine-tuning setting of a ViT-H/16_{448}. We reduce peak stochastic depth from 0.3 to 0.25. To fine-tune on iNat18, we found that a learning rate 1e-3 performs better than the 1e-4 used in the original work.

Table 27: Hyperparameters for fine-tuning on ImageNet-1K and iNat18 many-shot classification.

Parameter	Value
Epochs	50
Batch size	1024
Stochastic depth [37]	
Peak rate	0.2 (L/2B), 0.3 (H)
Decay	✓
Optimizer	AdamW [51, 42]
Learning rate	1e-3
Layer-wise lr decay [17]	0.75
Weight decay	0.05
Momentum	$\beta_1 = 0.9, \beta_2 = 0.999$
Freeze Blocks	0 (L/H), 6 (2B)
Learning rate schedule	linear warmup $\rightarrow$ cosine decay
Warmup epochs	5
End Learning Rate	1e-6
Label smoothing [68]	0.1

Parameter	Value
Train Data Augmentation	
`RandomResizedCrop`	224
`scale`	[0.08, 1.0]
`interpolation`	bicubic
`RandomHorizontalFlip`	$p = 0.5$
`RandAug [18]`	
`magnitude`	9
`magnitude_std`	0.5
`Normalize`	ImageNet statistics
`Mixup [84]` α	0.8
`Cutmix [84]` α	1.0
Test Data Augmentation	
`Resize`	256
`interpolation`	bicubic
`CenterCrop`	224
`Normalize`	ImageNet statistics

G.12 ADE20K Semantic Segmentation Fine-tuning

We fine-tune ViT-L models using an UperNet [78] segmentation head to predict a segmentation mask. We follow common practices and fine-tune on 512x512 resolution, where we interpolate the absolute positional embedding from 224x224 to 512x512, add relative position bias to the attention layers (initialized to 0) [30] and introduce layerscale [69] (initialized to 1). A common augmentation pipeline is used that consists of random rescaling, random horizontal flipping, color jitter and padding if necessary. We train for 160K updates using a batchsize of 16, a learning rate of 2e-5, weight decay 0.05, linear warmup for 1.5K update steps followed by cosine decay, stochastic depth rate 0.2, dropout 0.1, layer-wise learning rate decay 0.95. We evaluate after 160K update steps using a sliding window of 341 pixels and report mIoU over the validation set.

G.13 k-NN Classification and Semantic Segmentation Probe per Block

For the per-block analysis in Figure 3b and Figure 6 we follow the respective settings of k-NN classification (Appendix Section G.4) and semantic segmentation linear probing (Appendix Section G.9). The only change is that for semantic segmentation linear probing per-block, we fix the learning rate to 0.1 and only use the patch tokens of the respective block as input to the linear probe.

G.14 Loss Schedule Visualizatios

We visualize the schedules used for scheduling the loss weight of ID heads attached at intermediate blocks in the ablation study (Table 2) in Figure 9.

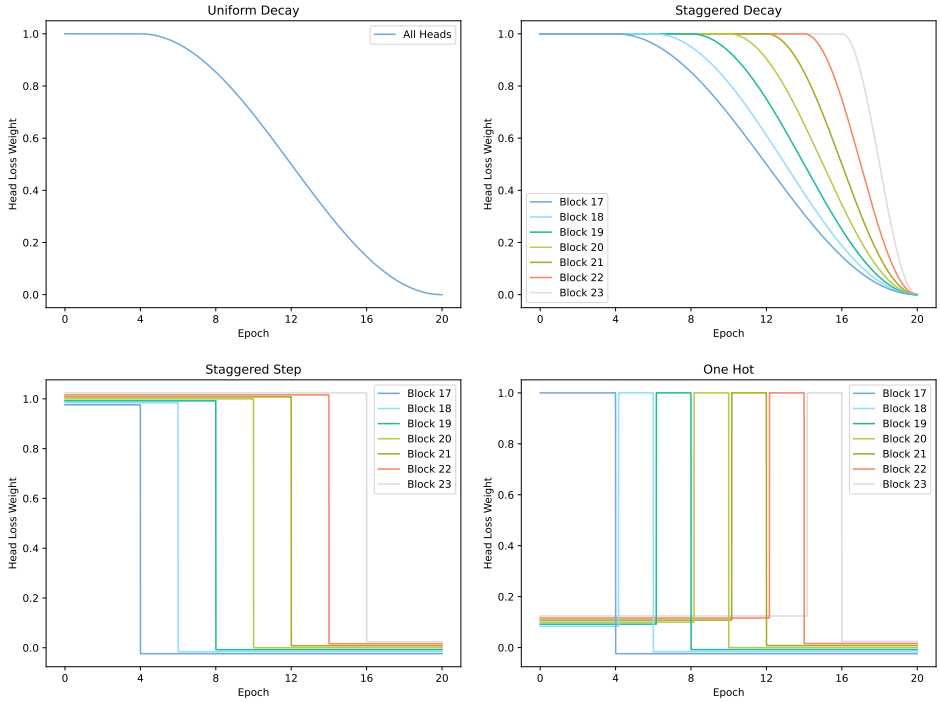

Figure 9: Loss weight schedules for the ablation in Table 2. For visual clarity, small offsets are added when values overlap (for "One Hot" and "Staggered Step").

H Relation to NNCLR

Figure 10 shows the difference between NNCLR [24] and NNA. NNCLR uses the NN-swap also for the negatives, resulting in a worse signal due to the NNs being retrieved from a FIFO queue of features from previous model states.

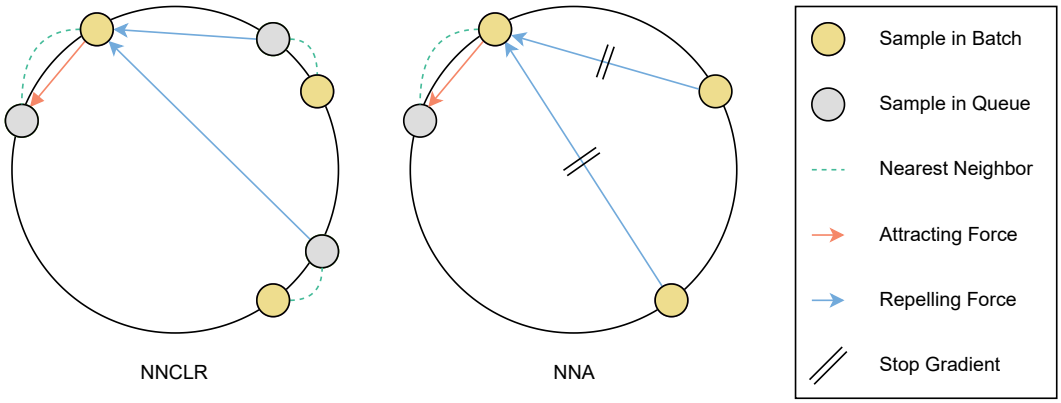

Figure 10: The NN-swap of NNCLR introduces inter-sample correlations between positives but uses features from a previous state of the model. Using the NN-swap only for the positives preserves the inter-sample correlations while using features from the current state of the model as negatives to improve the loss signal.

I Practitioner's Guide

We find MIM-Refiner to be easy to tune. By freezing the encoder and training multiple ID heads attached to the encoder with different hyperparameters, one can get a quick and cheap evaluation of suitable hyperparameters. We mainly use two metrics to judge the performance of an ID head:

- Accuracy of a k-NN classifier trained on a subset of the data (e.g. 10% of the data). This is relativley cheap to compute and can be done periodically during training. For the k-NN classifier, one can use either features of an encoder block or features of intermediate blocks in an ID head to judge the representation at the respective location in the network.
- The accuracy of the NN-swap, i.e. how often is the NN from the NN-swap from the same class as the query sample. This metric is essentially free to compute as the NN-swap is required for training anyways.

J Acknowledgements

We thank Johannes Lehner for helpful discussions and suggestions.

We acknowledge EuroHPC Joint Undertaking for awarding us access to Karolina at IT4Innovations, Czech Republic, MeluXina at LuxProvide, Luxembourg, LUMI at CSC, Finland and Leonardo at CINECA, Italy. We acknowledge access to LEONARDO at CINECA, Italy, via an AURELEO (Austrian Users at LEONARDO supercomputer) project.

The ELLIS Unit Linz, the LIT AI Lab, the Institute for Machine Learning, are supported by the Federal State Upper Austria. We thank the projects Medical Cognitive Computing Center (MC3), INCONTROL-RL (FFG-881064), PRIMAL (FFG-873979), S3AI (FFG-872172), EPILEPSIA (FFG-892171), AIRI FG 9-N (FWF-36284, FWF-36235), AI4GreenHeatingGrids (FFG- 899943), INTEGRATE (FFG-892418), ELISE (H2020-ICT-2019-3 ID: 951847), Stars4Waters (HORIZON-CL6-2021-CLIMATE-01-01). We thank Audi.JKU Deep Learning Center, TGW LOGISTICS GROUP GMBH, Silicon Austria Labs (SAL), FILL Gesellschaft mbH, Anyline GmbH, Google, ZF Friedrichshafen AG, Robert Bosch GmbH, UCB Biopharma SRL, Merck Healthcare KGaA, Verbund AG, GLS (Univ. Waterloo), Software Competence Center Hagenberg GmbH, Borealis AG, TÜV Austria, Frauscher Sensonic, TRUMPF and the NVIDIA Corporation.

NeurIPS Paper Checklist

1. **Claims**

   Question: Do the main claims made in the abstract and introduction accurately reflect the paper's contributions and scope?

   Answer: [Yes]

   Justification: We introduce MIM-Refiner, a method to refine pre-trained MIM models via an ensemble of contrastive heads.

   Guidelines:

   - The answer NA means that the abstract and introduction do not include the claims made in the paper.
   - The abstract and/or introduction should clearly state the claims made, including the contributions made in the paper and important assumptions and limitations. A No or NA answer to this question will not be perceived well by the reviewers.
   - The claims made should match theoretical and experimental results, and reflect how much the results can be expected to generalize to other settings.
   - It is fine to include aspirational goals as motivation as long as it is clear that these goals are not attained by the paper.

2. **Limitations**

   Question: Does the paper discuss the limitations of the work performed by the authors?

   Answer: [Yes]

   Justification: We discuss limitations in Section D, for example, the reliance on batch normalization.

   Guidelines:

   - The answer NA means that the paper has no limitation while the answer No means that the paper has limitations, but those are not discussed in the paper.
   - The authors are encouraged to create a separate "Limitations" section in their paper.
   - The paper should point out any strong assumptions and how robust the results are to violations of these assumptions (e.g., independence assumptions, noiseless settings, model well-specification, asymptotic approximations only holding locally). The authors should reflect on how these assumptions might be violated in practice and what the implications would be.
   - The authors should reflect on the scope of the claims made, e.g., if the approach was only tested on a few datasets or with a few runs. In general, empirical results often depend on implicit assumptions, which should be articulated.
   - The authors should reflect on the factors that influence the performance of the approach. For example, a facial recognition algorithm may perform poorly when image resolution is low or images are taken in low lighting. Or a speech-to-text system might not be used reliably to provide closed captions for online lectures because it fails to handle technical jargon.
   - The authors should discuss the computational efficiency of the proposed algorithms and how they scale with dataset size.
   - If applicable, the authors should discuss possible limitations of their approach to address problems of privacy and fairness.
   - While the authors might fear that complete honesty about limitations might be used by reviewers as grounds for rejection, a worse outcome might be that reviewers discover limitations that aren't acknowledged in the paper. The authors should use their best judgment and recognize that individual actions in favor of transparency play an important role in developing norms that preserve the integrity of the community. Reviewers will be specifically instructed to not penalize honesty concerning limitations.

3. **Theory Assumptions and Proofs**

   Question: For each theoretical result, does the paper provide the full set of assumptions and a complete (and correct) proof?

Answer: [NA]

Justification: No theoretical results.

Guidelines:

- The answer NA means that the paper does not include theoretical results.
- All the theorems, formulas, and proofs in the paper should be numbered and cross-referenced.
- All assumptions should be clearly stated or referenced in the statement of any theorems.
- The proofs can either appear in the main paper or the supplemental material, but if they appear in the supplemental material, the authors are encouraged to provide a short proof sketch to provide intuition.
- Inversely, any informal proof provided in the core of the paper should be complemented by formal proofs provided in appendix or supplemental material.
- Theorems and Lemmas that the proof relies upon should be properly referenced.

4. **Experimental Result Reproducibility**

   Question: Does the paper fully disclose all the information needed to reproduce the main experimental results of the paper to the extent that it affects the main claims and/or conclusions of the paper (regardless of whether the code and data are provided or not)?

   Answer: [Yes]

   Justification: We provide implementation details in Appendix F and provide the code that was used for this work in the supplemental materials. The code includes all exact run configurations used for training and evaluation.

   Guidelines:

   - The answer NA means that the paper does not include experiments.
   - If the paper includes experiments, a No answer to this question will not be perceived well by the reviewers: Making the paper reproducible is important, regardless of whether the code and data are provided or not.
   - If the contribution is a dataset and/or model, the authors should describe the steps taken to make their results reproducible or verifiable.
   - Depending on the contribution, reproducibility can be accomplished in various ways. For example, if the contribution is a novel architecture, describing the architecture fully might suffice, or if the contribution is a specific model and empirical evaluation, it may be necessary to either make it possible for others to replicate the model with the same dataset, or provide access to the model. In general. releasing code and data is often one good way to accomplish this, but reproducibility can also be provided via detailed instructions for how to replicate the results, access to a hosted model (e.g., in the case of a large language model), releasing of a model checkpoint, or other means that are appropriate to the research performed.
   - While NeurIPS does not require releasing code, the conference does require all submissions to provide some reasonable avenue for reproducibility, which may depend on the nature of the contribution. For example
     (a) If the contribution is primarily a new algorithm, the paper should make it clear how to reproduce that algorithm.
     (b) If the contribution is primarily a new model architecture, the paper should describe the architecture clearly and fully.
     (c) If the contribution is a new model (e.g., a large language model), then there should either be a way to access this model for reproducing the results or a way to reproduce the model (e.g., with an open-source dataset or instructions for how to construct the dataset).
     (d) We recognize that reproducibility may be tricky in some cases, in which case authors are welcome to describe the particular way they provide for reproducibility. In the case of closed-source models, it may be that access to the model is limited in some way (e.g., to registered users), but it should be possible for other researchers to have some path to reproducing or verifying the results.

5. **Open access to data and code**

Question: Does the paper provide open access to the data and code, with sufficient instructions to faithfully reproduce the main experimental results, as described in supplemental material?

Answer: [Yes]

Justification: We provide the code that was used for this work in the supplemental materials.

Guidelines:

- The answer NA means that paper does not include experiments requiring code.
- Please see the NeurIPS code and data submission guidelines (`https://nips.cc/public/guides/CodeSubmissionPolicy`) for more details.
- While we encourage the release of code and data, we understand that this might not be possible, so "No" is an acceptable answer. Papers cannot be rejected simply for not including code, unless this is central to the contribution (e.g., for a new open-source benchmark).
- The instructions should contain the exact command and environment needed to run to reproduce the results. See the NeurIPS code and data submission guidelines (`https://nips.cc/public/guides/CodeSubmissionPolicy`) for more details.
- The authors should provide instructions on data access and preparation, including how to access the raw data, preprocessed data, intermediate data, and generated data, etc.
- The authors should provide scripts to reproduce all experimental results for the new proposed method and baselines. If only a subset of experiments are reproducible, they should state which ones are omitted from the script and why.
- At submission time, to preserve anonymity, the authors should release anonymized versions (if applicable).
- Providing as much information as possible in supplemental material (appended to the paper) is recommended, but including URLs to data and code is permitted.

6. **Experimental Setting/Details**

   Question: Does the paper specify all the training and test details (e.g., data splits, hyperparameters, how they were chosen, type of optimizer, etc.) necessary to understand the results?

   Answer: [Yes]

   Justification: Appendix Section F lists implementation details and hyperparameters. Additionally, the code in the supplementary materials contains all exact run configurations.

   Guidelines:

   - The answer NA means that the paper does not include experiments.
   - The experimental setting should be presented in the core of the paper to a level of detail that is necessary to appreciate the results and make sense of them.
   - The full details can be provided either with the code, in appendix, or as supplemental material.

7. **Experiment Statistical Significance**

   Question: Does the paper report error bars suitably and correctly defined or other appropriate information about the statistical significance of the experiments?

   Answer: [No]

   Justification: Reruns on large-scale models are expensive. However, we report average performances in cheap benchmarks such as low-shot classification.

   Guidelines:

   - The answer NA means that the paper does not include experiments.
   - The authors should answer "Yes" if the results are accompanied by error bars, confidence intervals, or statistical significance tests, at least for the experiments that support the main claims of the paper.
   - The factors of variability that the error bars are capturing should be clearly stated (for example, train/test split, initialization, random drawing of some parameter, or overall run with given experimental conditions).

- The method for calculating the error bars should be explained (closed form formula, call to a library function, bootstrap, etc.)
- The assumptions made should be given (e.g., Normally distributed errors).
- It should be clear whether the error bar is the standard deviation or the standard error of the mean.
- It is OK to report 1-sigma error bars, but one should state it. The authors should preferably report a 2-sigma error bar than state that they have a 96% CI, if the hypothesis of Normality of errors is not verified.
- For asymmetric distributions, the authors should be careful not to show in tables or figures symmetric error bars that would yield results that are out of range (e.g. negative error rates).
- If error bars are reported in tables or plots, The authors should explain in the text how they were calculated and reference the corresponding figures or tables in the text.

8. **Experiments Compute Resources**

   Question: For each experiment, does the paper provide sufficient information on the computer resources (type of compute workers, memory, time of execution) needed to reproduce the experiments?

   Answer: [Yes]

   Justification: We report used compute resources in Appendix Section F.2 and compare runtimes to train models in Figure 2.

   Guidelines:

   - The answer NA means that the paper does not include experiments.
   - The paper should indicate the type of compute workers CPU or GPU, internal cluster, or cloud provider, including relevant memory and storage.
   - The paper should provide the amount of compute required for each of the individual experimental runs as well as estimate the total compute.
   - The paper should disclose whether the full research project required more compute than the experiments reported in the paper (e.g., preliminary or failed experiments that didn't make it into the paper).

9. **Code Of Ethics**

   Question: Does the research conducted in the paper conform, in every respect, with the NeurIPS Code of Ethics `https://neurips.cc/public/EthicsGuidelines`?

   Answer: [Yes]

   Justification: Our paper conforms with the guidelines.

   Guidelines:

   - The answer NA means that the authors have not reviewed the NeurIPS Code of Ethics.
   - If the authors answer No, they should explain the special circumstances that require a deviation from the Code of Ethics.
   - The authors should make sure to preserve anonymity (e.g., if there is a special consideration due to laws or regulations in their jurisdiction).

10. **Broader Impacts**

    Question: Does the paper discuss both potential positive societal impacts and negative societal impacts of the work performed?

    Answer: [NA]

    Justification: -

    Guidelines:

    - The answer NA means that there is no societal impact of the work performed.
    - If the authors answer NA or No, they should explain why their work has no societal impact or why the paper does not address societal impact.

- Examples of negative societal impacts include potential malicious or unintended uses (e.g., disinformation, generating fake profiles, surveillance), fairness considerations (e.g., deployment of technologies that could make decisions that unfairly impact specific groups), privacy considerations, and security considerations.
- The conference expects that many papers will be foundational research and not tied to particular applications, let alone deployments. However, if there is a direct path to any negative applications, the authors should point it out. For example, it is legitimate to point out that an improvement in the quality of generative models could be used to generate deepfakes for disinformation. On the other hand, it is not needed to point out that a generic algorithm for optimizing neural networks could enable people to train models that generate Deepfakes faster.
- The authors should consider possible harms that could arise when the technology is being used as intended and functioning correctly, harms that could arise when the technology is being used as intended but gives incorrect results, and harms following from (intentional or unintentional) misuse of the technology.
- If there are negative societal impacts, the authors could also discuss possible mitigation strategies (e.g., gated release of models, providing defenses in addition to attacks, mechanisms for monitoring misuse, mechanisms to monitor how a system learns from feedback over time, improving the efficiency and accessibility of ML).

11. **Safeguards**

    Question: Does the paper describe safeguards that have been put in place for responsible release of data or models that have a high risk for misuse (e.g., pretrained language models, image generators, or scraped datasets)?

    Answer: [NA]

    Justification: -

    Guidelines:

    - The answer NA means that the paper poses no such risks.
    - Released models that have a high risk for misuse or dual-use should be released with necessary safeguards to allow for controlled use of the model, for example by requiring that users adhere to usage guidelines or restrictions to access the model or implementing safety filters.
    - Datasets that have been scraped from the Internet could pose safety risks. The authors should describe how they avoided releasing unsafe images.
    - We recognize that providing effective safeguards is challenging, and many papers do not require this, but we encourage authors to take this into account and make a best faith effort.

12. **Licenses for existing assets**

    Question: Are the creators or original owners of assets (e.g., code, data, models), used in the paper, properly credited and are the license and terms of use explicitly mentioned and properly respected?

    Answer: [Yes]

    Justification: Authors of code, data and models are cited accordingly.

    Guidelines:

    - The answer NA means that the paper does not use existing assets.
    - The authors should cite the original paper that produced the code package or dataset.
    - The authors should state which version of the asset is used and, if possible, include a URL.
    - The name of the license (e.g., CC-BY 4.0) should be included for each asset.
    - For scraped data from a particular source (e.g., website), the copyright and terms of service of that source should be provided.
    - If assets are released, the license, copyright information, and terms of use in the package should be provided. For popular datasets, `paperswithcode.com/datasets` has curated licenses for some datasets. Their licensing guide can help determine the license of a dataset.

- For existing datasets that are re-packaged, both the original license and the license of the derived asset (if it has changed) should be provided.
- If this information is not available online, the authors are encouraged to reach out to the asset's creators.

13. **New Assets**

    Question: Are new assets introduced in the paper well documented and is the documentation provided alongside the assets?

    Answer: [Yes]

    Justification: Details on how the new models were trained are described in the paper.

    Guidelines:

    - The answer NA means that the paper does not release new assets.
    - Researchers should communicate the details of the dataset/code/model as part of their submissions via structured templates. This includes details about training, license, limitations, etc.
    - The paper should discuss whether and how consent was obtained from people whose asset is used.
    - At submission time, remember to anonymize your assets (if applicable). You can either create an anonymized URL or include an anonymized zip file.

14. **Crowdsourcing and Research with Human Subjects**

    Question: For crowdsourcing experiments and research with human subjects, does the paper include the full text of instructions given to participants and screenshots, if applicable, as well as details about compensation (if any)?

    Answer: [NA]

    Justification: -

    Guidelines:

    - The answer NA means that the paper does not involve crowdsourcing nor research with human subjects.
    - Including this information in the supplemental material is fine, but if the main contribution of the paper involves human subjects, then as much detail as possible should be included in the main paper.
    - According to the NeurIPS Code of Ethics, workers involved in data collection, curation, or other labor should be paid at least the minimum wage in the country of the data collector.

15. **Institutional Review Board (IRB) Approvals or Equivalent for Research with Human Subjects**

    Question: Does the paper describe potential risks incurred by study participants, whether such risks were disclosed to the subjects, and whether Institutional Review Board (IRB) approvals (or an equivalent approval/review based on the requirements of your country or institution) were obtained?

    Answer: [NA]

    Justification: -

    Guidelines:

    - The answer NA means that the paper does not involve crowdsourcing nor research with human subjects.
    - Depending on the country in which research is conducted, IRB approval (or equivalent) may be required for any human subjects research. If you obtained IRB approval, you should clearly state this in the paper.
    - We recognize that the procedures for this may vary significantly between institutions and locations, and we expect authors to adhere to the NeurIPS Code of Ethics and the guidelines for their institution.
    - For initial submissions, do not include any information that would break anonymity (if applicable), such as the institution conducting the review.